1. Introduction

The radioactive noble gas ^{85}Kr is a beta emitter with a half-life of 10.76 years. Natural ^{85}Kr is produced by nuclear reactions by cosmic radiation in the upper atmosphere and spontaneous fission of the heavy elements in the Earth's crust (Styra and Butkus, 1991).

However most of the ^{85}Kr in the present atmosphere is derived from anthropogenic sources (i.e., nuclear weapons tests, nuclear-fuel reprocessing plants and nuclear reactors). At present, the major sources of atmospheric ^{85}Kr are releases from the nuclear fuel reprocessing plants in Europe (Rath, 1988, Von Hippel et al., 1986, Weiss et al., 1986 and 1992).

The relatively well-known distribution of the point like sources and the fact that the only significant sink in the atmosphere is radioactive decay, make ^{85}Kr an ideal tracer to assess the characteristics of the large-scale horizontal and the interhemispheric transport, as depicted in numerical atmospheric circulation models. For instance Jacob et al. (1987), Zimmermann et al. (1989) and Draxler (2007) simulated the global ^{85}Kr distribution using a three-dimensional tropospheric model while Rath (1988) used a two-dimensional model.

The solubility of ^{85}Kr (as with all inert gases) in water is very low (the ratio of stable Kr to water is 1.85×10^{10} g/g at equilibrium) and therefore the ocean dissolves not more than 0.1% of the annual input of ^{85}Kr (Izrael et al., 1982). However ^{85}Kr is also a very useful tracer to have better understanding of oceanic processes such as relatively short-term (decadal) atmosphere-ocean exchanges and the determination of the age distribution of water masses in the ocean as described by Loosli (1992). The ^{85}Kr distribution in the atmosphere can also be used as an indicator of clandestine separation of plutonium for building nuclear weapons.

Because of its inertness, the major sink of ^{85}Kr in the Earth's surface is a radioactive decay at the rate of about 6% per year. The imbalance between sinks and sources of ^{85}Kr causes a change in the atmospheric ^{85}Kr global inventory. The current global inventory of ^{85}Kr in the atmosphere is estimated to be 5000 PBq (Hirota et al., 2004). Thus, 300 PBq of ^{85}Kr has been lost each year from the atmosphere, due to its radioactive decay. However, the amount of released ^{85}Kr from the nuclear-fuel reprocessing plants in Europe is now 300 to 400 PBq per year（United Nations, 2000). In fact the atmospheric ^{85}Kr activity concentration is increasing yearly according to the differences between released ^{85}Kr and decayed ^{85}Kr (Hirota et al., 2004; Igarashi et al., 2000; Pollard et al., 1997).

Owing to its long half-life and chemically inertness, ^{85}Kr has spread all over the globe. The activity concentration of ^{85}Kr in ground level air of 1.3 Bq m^{-3} in 1999 at mid-latitudes of the Northern Hemisphere is slowly but continuously increasing at an annual rate of 30 mBq m^{-3} because the annual global release rate of ^{85}Kr to the atmosphere still exceeds the removal rate by decay. Therefore it is important to monitor the concentration of atmospheric ^{85}Kr in order to evaluate potential radioecological impacts on human health and the environment. Regarding radiation protection, based on its small effective dose conversion factor of the order of nSv yr^{-1} per Bq m^{-3}, the annual dose of ^{85}Kr received by the general public is insignificant compared with the annual external dose from natural sources. In the vicinity of a nuclear-fuel reprocessing plant the ^{85}Kr activity concentrations sometimes reach values of some hundred thousand Bq m^{-3} for a short period of time (Gurriaran et al., 2004). Even in this case the average ^{85}Kr activity concentration over a year would not reach the proposed ICRP dose limit (Fujitaka, 1995). From the viewpoint of the atmospheric sciences ^{85}Kr data can be used for validation of local, regional and global transport models. The well-known source term and its chemically inert properties

make ^{85}Kr a useful tool for atmospheric studies (Weiss et al., 1986, 1987, 1992) in which transport and dilution processes should be considered but no complicated chemical reactions are involved. In addition it seems possible to detect clandestine plutonium production for nuclear weapons by monitoring ^{85}Kr (Sittkus and Stockburger, 1976, Kalinowski et al., 2004, World Meteorological Organization, 1996). As an environmental effect the contribution of ^{85}Kr to air conductivity has been discussed (Styra and Butkus, 1991; Stockburger et al., 1977), although the contribution of ^{85}Kr at background concentration levels is concluded to be much smaller than the natural ones and to be buried in natural fluctuations. However, attention should be given to the fact that the background level of the atmospheric ^{85}Kr activity concentration at the global level is still increasing.

At the Meteorological Research Institute (MRI) in Tsukuba, Japan, atmospheric ^{85}Kr activity concentrations have been observed since 1995 in collaboration with the Bundesamt für Strahlenschutz (BfS), Germany (Igarashi et al., 2000). Igarashi et al. (2001) developed a ^{85}Kr measuring system based on the BfS method in 2000. Details of the method and the techniques developed and used by the BfS to monitor the activity concentrations of ^{85}Kr and ^{133}Xe are described in Stockburger et al., 1977 and in Sartorius et al. 2002. It was confirmed by intercomparison measurements between the BfS and the MRI laboratories that the ^{85}Kr activity concentration measured by the MRI system is traceable to the value determined by the BfS. (Igarashi et al., 2001, Figure 8, see appendix 4)

In 2006 the MRI and the Japan Chemical Analysis Center (JCAC) conducted a cooperative research program of 18 months to develop a practical ^{85}Kr measuring system based on the MRI system. The objectives of this program were to establish a monitoring system of atmospheric ^{85}Kr in Japan and to publish a technical document on ^{85}Kr measurements.

In this technical report we describe the ^{85}Kr measurement system and report the results of 10 years of observation of ^{85}Kr in Tsukuba, Japan.

2. Instruments of cold charcoal trap - gas chromatography - gas counting system of ^{85}Kr

In this chapter we describe the sampling procedures, including a sampling apparatus (cold charcoal trap), and the determination of ^{85}Kr activity concentration by a combined gas chromatography and gas counting system as well as the description of the instrumentation.

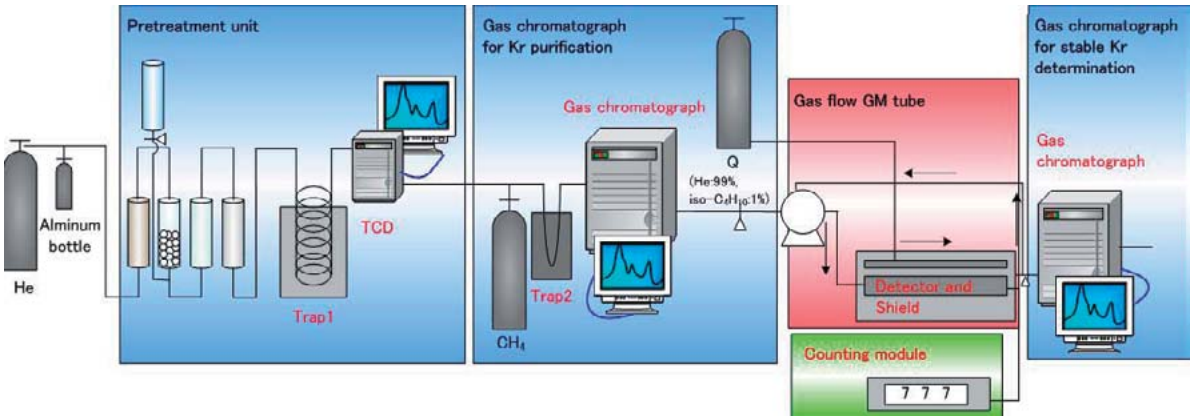

Figure 2.1 Schematic diagram of the ^{85}Kr measurement system

2.1 Sampling procedures

2.1.1 Outline

Atmospheric krypton is collected using a sampling apparatus (Fig. 2.2) that consists of an air pump, a metal absorber, and a liquid nitrogen dewar bottle. First the air is passed through a glass filter (Whatman GF/F 47mmØ) to remove dust, and then dehumidified with a refrigerator or a dehumidifier. After removal of dust and water vapor the air is passed through a metal absorber, which is immersed in a liquid nitrogen dewar using the air pump and the atmospheric Kr is trapped on the activated charcoal that fills the lower part of the absorber. Air sampling is continuously performed for one week at a constant flow rate of 1

l min^{-1} and about 10 m^3 of the air is introduced into the absorber during the routine sampling period. After end of collection trapped moisture is removed from the absorber, and the absorber is heated to desorb the Kr trapped on the activated charcoal. The Kr fraction is completely transferred by expansion into an evacuated aluminum bottle followed by rinsing the absorber and the tubing with pressurized He gas at the end of the desorption step.

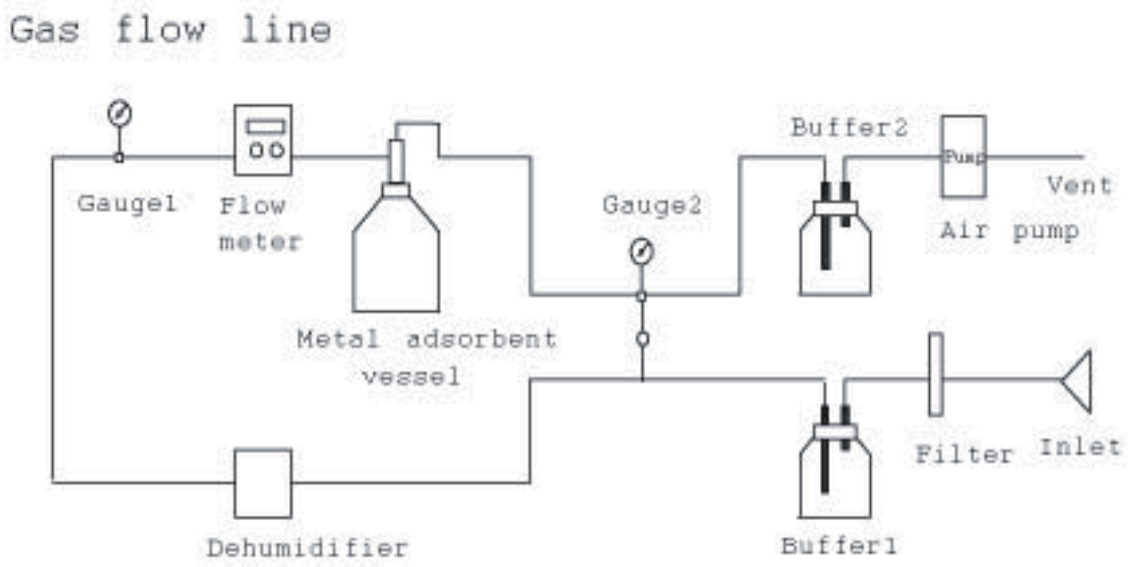

Figure 2.2 Diagram of sampling apparatus

The sampling procedure described below is based on the techniques and methods of the BfS, except for using refrigerator or a dehumidifier to remove moisture due to high humidity of the air in Japan. The metal absorber (Fig. 2.3) was developed and designed at the BfS (Sartorius et al. 2002, BfS 2004). It is cylindrical, 63cm and 6cmØ in length and in radius, respectively. The absorber has a needle valve, a stopcock, a manometer and a safety valve. The air flow rate through the absorber is regulated with a needle valve installed at the entrance of the absorber. Atmospheric Kr trapped on the activated charcoal is

transferred to an aluminum bottle by opening the stopcock at the outlet side of the absorber. The pressure in the absorber can be read by the manometer. When the pressure in the absorber exceeds +0.5 MPa, the excess pressure is automatically blown off through the safety valve. The upper part of the absorber internal volume has plenty of metal fins to remove from the air moisture as ice and CO_2 as dry ice. The lower part of the absorber internal volume is filled with 200 g of activated charcoal (No. 1.09631.0500, 0.3-0.5 mm (35-50 mesh), Merck, Germany). Atmospheric trace constituents with low melting points (e.g., Kr and Xe) are adsorbed on the activated charcoal at liquid nitrogen temperature. The absorber is kept at low pressure (about 0.5 atm) during sampling to avoid the condensation of the main air constituents N_2 and O_2. The major part of the air passed through the absorber is discharged by the air pump.

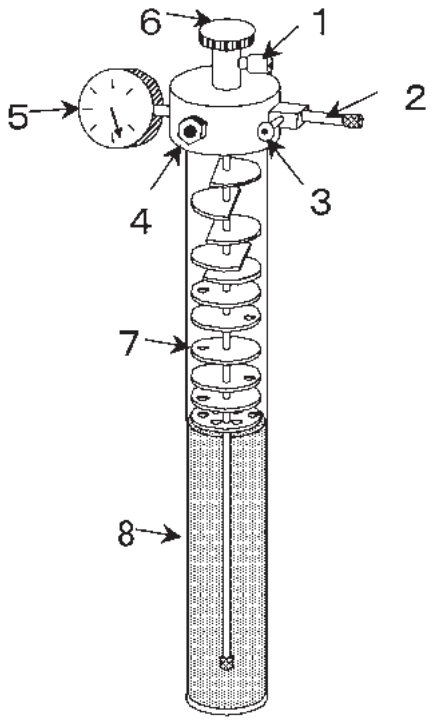

Figure 2.3 Absorber for ^{85}Kr sampling
1: Quick connects (sample out), 2: Quick connects (sample in), 3: Needle valve, 4: Safety valve, 5: Manometer, 6: Stop cock, 7: Fin, 8: Activated charcoal.

After collection, the absorber is warmed to room temperature. In this step, most of the gaseous air components (N_2, O_2 and CO_2) and the water are discharged from the absorber. The Kr trapped on the activated charcoal is transferred into an evacuated aluminum bottle (minican) by heating the absorber up to 300 ºC. Last of all the transfer is completed by sweeping the absorber and the tubings with He gas and flush the gas into the aluminium bottle at a pressure of 0.4 MPa. The aluminum bottle has a volume of about 1 l with a spring-type valve. Usually, this spring-type valve seals the aluminum bottle. When the spring-type valve is pushed with a thin stick, the spring can be depressed downward and the gas sample can be introduced into the aluminum bottle. The aluminum bottle can be covered with a cap to protect the valve. This lightweight but strong bottle is a suitable transportation container, and the gas sample can be preserved for a long period.

2.1.2 Start of sampling

To start sampling, fix the air inlet tube carefully to the outside wall of a building to avoid rainwater. Fresh air should be collected to ensure that the sample represents ^{85}Kr activity concentration in the atmosphere. During storage the absorber is kept under He pressure at +0.4 MPa. Before start of sampling the absorber is depressurized to atmospheric pressure by opening the stopcock at the outlet. Afterwards the stopcock is closed and the needle valve checked if its closed correctly. Attach the fixing rubber collar to the absorber and cool it in the liquid nitrogen dewar. Make sure approx. 10 cm of the stainless steel part of the absorber is above the top of the liquid nitrogen dewar. The screw bolt to exchange the activated charcoal is fitted on the bottom of the absorber. Any shocks may affect the air tightness of the absorber. Therefore, the handling of the absorber has to be paid care. In order to avoid that moisture in the air sticks on the surface of the absorber as ice and to

control the liquid nitrogen evaporation, it is required that the absorber is covered by a thermal insulator on the part of the fixing rubber collar. When the absorber is cooled by the liquid nitrogen, the activated charcoal firstly acts as a cryopump, and therefore the pressure of manometer is gradually decreased. The pressure of manometer will be constant, when the gas adsorption on the activated charcoal will be reached saturation. Connect the tubes to the absorber and turn on the flow meter. After the pressure of the manometer reached -0.06 MPa open the needle valve and adjust the flow rate to 1.00 l min^{-1}. Ten minutes later, turn on the air pump and open the stopcock completely.

2.1.3 Routine work during sampling

During sampling check the gauges (manometer, gauge1 and gauge2), flow rate, total air volume, and amount of remaining liquid nitrogen daily. Make sure that the pressure of the manometer is below -0.03 MPa, that the gauge1 constantly indicates the atmospheric pressure, and that gauge2 constantly indicates the negative pressure. It is important that the flow rate shows 1.00 l min^{-1}. When the flow rate is lower adjust the flow rate back to 1.00 l min^{-1} by opening the needle valve. The total amount of the air volume would be 1.44 m^3 per day.The consumption rate of liquid nitrogen is 3 to 5 kg per day, so refill the dewar with liquid nitrogen every two days. Due to the large thermal capacity of the absorber, its increase of the temperature is negligible if the absorber is taken out of liquid nitrogen dewar during the short time of refilling. But it is better to immerse the absorber into a spare liquid nitrogen dewar when refill the engaged dewar with liquid nitrogen.

2.1.4 Exchange of the absorber

At the end of the collection period close the stopcock and the needle valve of the

absorber in use and turn off the air pump. Disconnect the tubes from the absorber, take it out of the dewar and remove the rubber collar from the absorber. Turn the absorber upside down and hold it in a stand (refer to Fig. 2.4). When the pressure in the absorber has been above atmospheric pressure (it takes about 5 minutes), open the stopcock completely and leave it for 35 minutes. During this time the main air components adsorbed on the activated charcoal are discharged. We determined that 1-2 % of Krypton had lost during a one hour warming up. In case the stopcock has not been opened when warming up the absorber to room temperature, the pressure in the absorber increases over +0.5 MPa, the safety valve is automatically opened and the pressure in the absorber is immediately decreased. Exchange a glass filter of the sample unit and refill the dewar with liquid nitrogen. Finally start the next sampling with the other absorber as described in chapter 2.1.2 “Start of sampling”.

Figure 2.4 Removal of water from absorber

2.1.5 Transfer Kr to aluminum bottle

Close the stopcock of the upside down absorber and leave it stand again for one hour to dissolve the ice trapped in the absorber. The pressure in the absorber increases to +0.2 MPa due to the desorption of air trapped on the activated charcoal. If the pressure in the absorber is less than +0.04 MPa, pressurize it with He gas to +0.1 MPa. Rotate the absorber, which is turned upside down, like a top, attach the Quick-connects (Swagelok®) to the port of the needle valve, open the needle valve and allow the water, trapped in the absorber, run out dropwise into a beaker. Recording the amount of water can help determine whether the moisture trap in the absorber is operating correctly or not.

After the pressure of the absorber reaches atmospheric pressure close the needle valve, remove the Quick-connects and insert the absorber into a cylindrical heater. When the sample gas is transferred into the aluminum bottle, use a water adsorbent tube to remove the water vapor in the sample gas (Figures.2.5 and 2.6). Fill the inner tube of the water adsorbent tube with the regenerated silica gels, insert it into the outer tube, and connect it firmly to the upper cap of the water adsorbent tube with the stretching ring. The water adsorbent tube is connected between the absorber and the aluminum bottle. When the water adsorbent tube is assembled no silica gel should remain on the surface of the flange of the inner tube.

Figure 2.5 Water adsorbent tube

Figure 2.6 Transfer of sample gas

Screw a closed minican valve onto an evacuated aluminum bottle (minican), and connect it to the water adsorbent tube with Quick-connects. Connect the counter-port of the water adsorbent tube to the absorber with the Quick-connects. Open the stopcock and the minican valve completely ensure that the manometer indicates negative pressure (-0.03 MPa) and then record it. Close both valves and switch on the heater. Heat the absorber for one hour at 300 ºC. Fifteen minutes after the heater was switched on check the manometer to make sure that no sharp increase of the pressure has occurred due to the water vapor. Open the stopcock and the minican valve completely to decrease the pressure of the system to constant pressure. After the stabilisation of the pressure in the system close both valves. After one hour open the stopcock and the minican valve completely and record the pressure of the manometer. The pressure of the gases in the minican is typically +0.1 - +0.3 MPa. To ensure a quantitative transfer of the desorbed gases from the activated charcoal to the aluminum bottle, rinse out the absorber by slowly pressurizing the system with He gas from the port of the needle valve side until +0.4 MPa is reached. After pressurizing at +0.4 MPa, close all the valves and remove the water adsorbent tube (including the minican valve and the aluminum bottle) from the absorber. Remove the minican valve (including the aluminum bottle) from the water adsorbent tube. Remove the aluminum bottle from the minican valve. Paste a sampling label on the bottle indicating the sampling location, the sampling period, and the sample number and then screw a cap onto the bottle.

2.1.6 Re-use of sampling instruments

a. Regeneration of the absorber

Connect a silicon tube to the outlet port of the stopcock side and open it to exhaust the excess pressure. At this time, water drops are attached inside the silicon tube. Blow He gas

into the absorber from the port of the needle valve side at a low flow rate. It is easy to adjust the flow rate by controlling the out-coming gas using a conventional flow meter with a water tube (at several bubbles per second). Continue to heat the absorber (300 ºC) until no condensed water is visible in the silicon tube at the outlet (about one hour).

Next, switch off the heater and leave the absorber in the heater for two hours. Continue to flush the absorber with He gas. After two hours close all the valves of the absorber, remove it from the heater, place it on the stand and allow it to cool. After the absorber is cooled to room temperature, pressurize it with He gas until +0.4 MPa is reached. Check the air tightness of the absorber by appling soapy water to the parts where leakage would occur making sure no bubbles appear. With the next usage of the absorber, air tightness can be ensured by maintaining the pressure (+0.4MPa).

b. Ensuring dryness of the water adsorbent tube

Open the stretching ring, remove the inner tube and move the silica gel to a beaker. Next regenerate the silica gel by heating it in a drying oven, dismantle the water adsorbent tube and dry the components until the next usage.

2.1.7 Maintenance

If a suitable flow rate can not be achieved during sampling, it is necessary to confirm that the air inlet has not been blocked. If the manometer has not maintained negative pressure, make sure that no leakage is occurring in the sampling unit and that the air pump has normal suction. If the air pump has failed, replace it with a spare air pump. If the exchanged air pump is repaired, it can be reused.

If the flow rate is unstable, check the connection between the tubes and the sampling unit. The activated charcoal in the absorber will become fine during use, and part of the

activated charcoal may flow out with water from the needle valve. Therefore, change the activated charcoal every one or two years.

2.2 A brief system description

The MRI ^{85}Kr measuring system consists of two trap tubes (made of stainless steel; Traps 1 and 2, packed with activated charcoal), three gas chromatographs (GC 1, 2 and 3) (GC-14B, Shimadzu, Kyoto, Japan), an activity measurement unit containing a gas-flow proportional counter (200 ml in volume) (No. 49583, LND, New York, USA) and two data processing and control systems (Shimadzu Chromatopack C-R7A). The sample flow lines are built mostly of using stainless-steel tubes (1/8 inch or 2 mm diameter) and connected by appropriate stainless-steel fittings (Swagelok, Solon, OH, USA and Shimadzu). The treatment unit (Shimazu) is composed of Trap 1 [6 mm diameter, filling: 60 ml of activated charcoal, 30 to 45 mesh (Shimadzu)] and a thermal conductivity detector (TCD; hereafter referred to as TCD-P). This unit is used for the crude separation of Kr from other gases. Figs. 2.7 and 2.8 show the schematic flow chart of pre-treatment unit and the GCs, respectively. The separation and purification conditions of the whole system were adjusted and calibrated by using simulated standard gas, which was designed to have a composition similar to that of the real sample gas in the aluminum bottle. The pre-treatment unit has multiple ports to introduce the simulated gas for test and calibration and He gas for purging the line; their amounts and flow rates are controlled by a mass flow monitor/controller (DS-3, Stech, Kyoto, Japan).

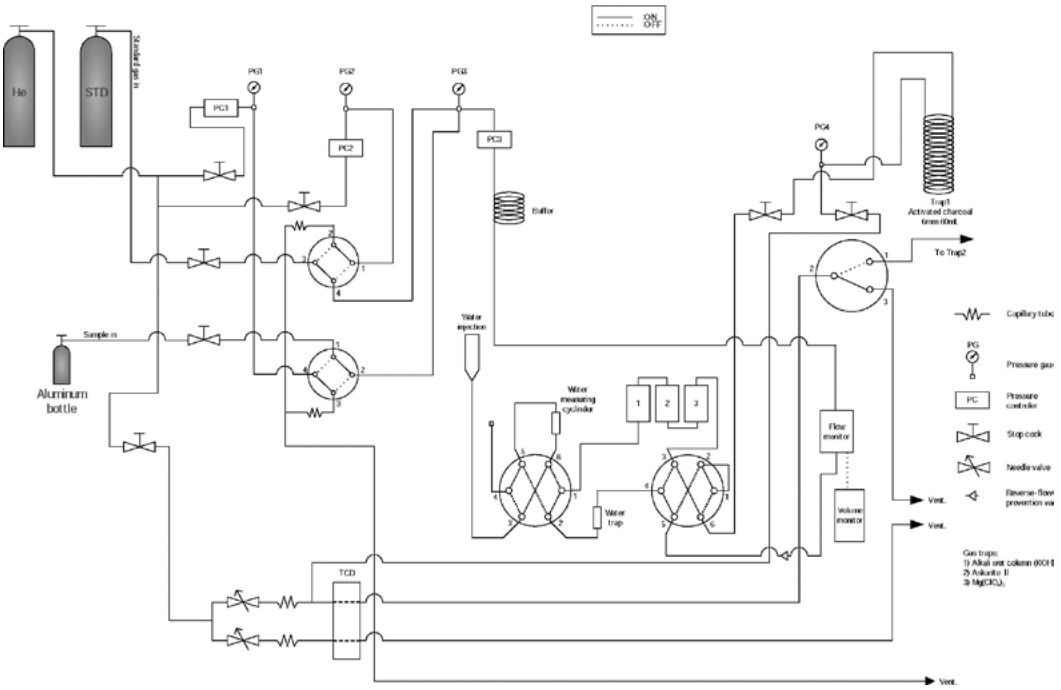

Figure 2.7 Schematic flow chart of pre-treatment unit

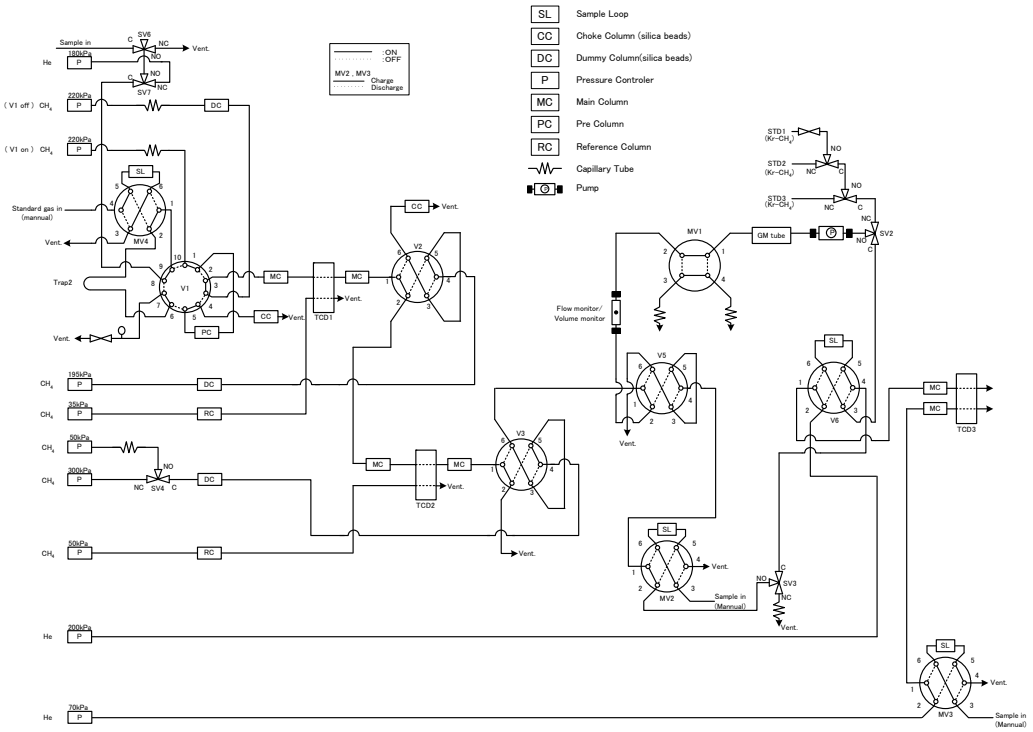

Figure 2.8 Schematic flow chart of the GCs

2.3 Analytical procedures

The sample gas in the aluminum bottle is injected into the pre-treatment unit (see Fig. 2.7); in the first stage, it sequentially passes through the wet CO_2 removal column and the water removal column. The wet CO_2 removal column (22 mm in diameter, 230 mm in length) has a special design to remove a large volume of CO_2; packed with Askarite II (No. C049-H40, 8-20 mesh, 50 g, Thomas Scientific, Swedesboro, NJ, USA), on the silica gel layer (0.35 to 2.0 mm, 7 g) (Kanto Kagaku, Tokyo, Japan), with 10 ml of pure water added just before the analysis. The water removal column (10 mm in diameter, 145 mm in length) is packed with $Mg(ClO_4)_2$ (No. 500-94444, 10 g) (Kishida Chemical, Osaka, Japan). The sample gas is pushed into the pre-treatment unit by over pressure in the aluminum bottle. The gas flow rate is set at 250 ml min^{-1} for the sample and at 350 ml min^{-1} for the simulated sample. The sample gas then flows into Trap 1 where it is cooled to -90 ºC by immersion in refrigerated ethanol (5 liter). The refrigerator used is a Cryocool CC-100II (Neslab, Portsmouth, NH, USA). After most of the sample gas is released in the aluminum bottle by over pressure, He gas is charged into the aluminum bottle to rinse it and to complete the sample transfer. The flush of pure He completely elutes major air components adsorbed on the activated charcoal in Trap 1 chromatographically. It usually takes 30 to 40 min to elute most of the air components from Trap 1. Fifty to 60 minutes after the start, Trap 1 is manually removed from the cold bath and placed in the heater (ARF-80KC, Asahi Rika, Chiba, Japan). Continuous He flow at up to 400 ºC transfers the gases retained in Trap 1 to Trap 2 (4 mm in diameter; filled with 1 ml of activated charcoal) immersed in liquid Ar (about 0.5 l). After adsorption of Kr in Trap 2, the trap is heated by a sheath heater, and the gases retained in the trap are injected sequentially into GC 1 and GC 2 for isolation of Kr (Fig. 2.8). In these processes, pure CH_4 (purity 99.999%) is used as a carrier

gas which is also used as part of the counting gas mixture in the proportional counter to improve the counting conditions for the ^{85}Kr activity measurement. The analytical conditions for the GCs are summarized in Table 1 in Igarashi et al., (2001). In addition, Trap 2 and GC 1, 2 and 3 are operated automatically by a Shimadzu Chromatopack C-R7A system and its BASIC program. The chromatogram output data of all GCs are automatically recorded and analyzed by the C-R7A.

The separation system at the Bundesamt für Strahlenschutz in Freiburg is based on two large-diameter, column and valve. It operates under normal pressure and a low gas flow rate of several milliliters per minute (Stockburger et al., 1977). The MRI separation system is composed of commercially available GC parts, (i.e., small-diameter tube, column and valve). It operates at relatively high pressures up to 300 kPa and a high gas flow rate of 70 ml min^{-1}. This caused a problem in the early version of the MRI system. Even if CO_2 were completely removed, the separation column was saturated with abundant N_2 and O_2 relative to Kr in the sample, resulting in insufficient isolation and purification of Kr from major air components. In the early stages of system development, removal of O_2 was attempted by using an oxidation reaction column, but a satisfactory outcome was not obtained. Therefore, the idea of chemical removal of O_2 was later rejected. A pre-treatment unit, which employed gas chromatographic separation at low temperature, was newly developed and integrated. Crude separation of Kr from N_2 and O_2 is carried out with this unit, to achieve the complete isolation of Kr. This unit is the most innovative part of the MRI system. Activated charcoal, which has a high affinity to noble gases heavier than Ar was chosen as an adsorbent in this trap-and-purge technique. Trap 1 was also intended to have a sufficiently large capacity (60 ml) to avoid saturation problems. In order to achieve the chromatographic separation of N_2 and O_2 from the noble gas fraction, the retention time

of Kr at low temperature was monitored. A known volume of Kr was introduced into Trap 1 immersed in a different cold medium and its elution was recorded. The retention time was increased to a good value by decreasing the column temperare. The retention time of Kr was long enough to completely separate Kr from other gas components at 90 ºC. It was also confirmed that the temperature for the purge procedure should be as high as possible so as to ensure the recovery of the noble gas fraction from the trap. In practice, the purge temperature was set at 400 ºC.

2.4 Gas counting system

The purified Kr fraction is subsequently introduced into the loop which includes the proportional conter (Fig. 2.9). The loop is closed off after the Kr fraction has been introduced and the sample gases in the loop are mixed well by circulation with a newly devised plunger-type air pump (Mac pump 40, Nitto Koatsu, Ibaraki, Japan) in order to attain homogeneity in the loop. When homogeneity has been achieved, the excess pressure is released by equilibration with atmospheric pressure through a four-way valve in the loop. The beta activity of ^{85}Kr is counted by the proportional counter. Background counting is carried out before and after the Kr sample measurement to confirm the sample purge. The beta-counting of ^{85}Kr is continued until at least 10000 net counts have been obtained. The activity counting unit is composed of a NIM bin power module (Repic RPN-011), a four-channel high-voltage supply (Repic RPH-011), a pre-amplifier (Model 142AH, Ortec, Tennessee, USA), an analog-to-digital converter (Model 705, Philips Scientific, Mahwah, NJ, USA), a gate and delay generator (Model 794, Philips Scientific), logics devices (Models 756 and 757, Philips Scientific), and a personal computer support counter system (RPN-032, Repic). Along with activity counting, the volume of stable Kr in the loop is

precisely determined with GC 3, the sampling loop of which is also located in the above-mentioned recirculating loop. Thus the specific activity of ^{85}Kr is obtained from the activity counting and the stable Kr volume measurements.

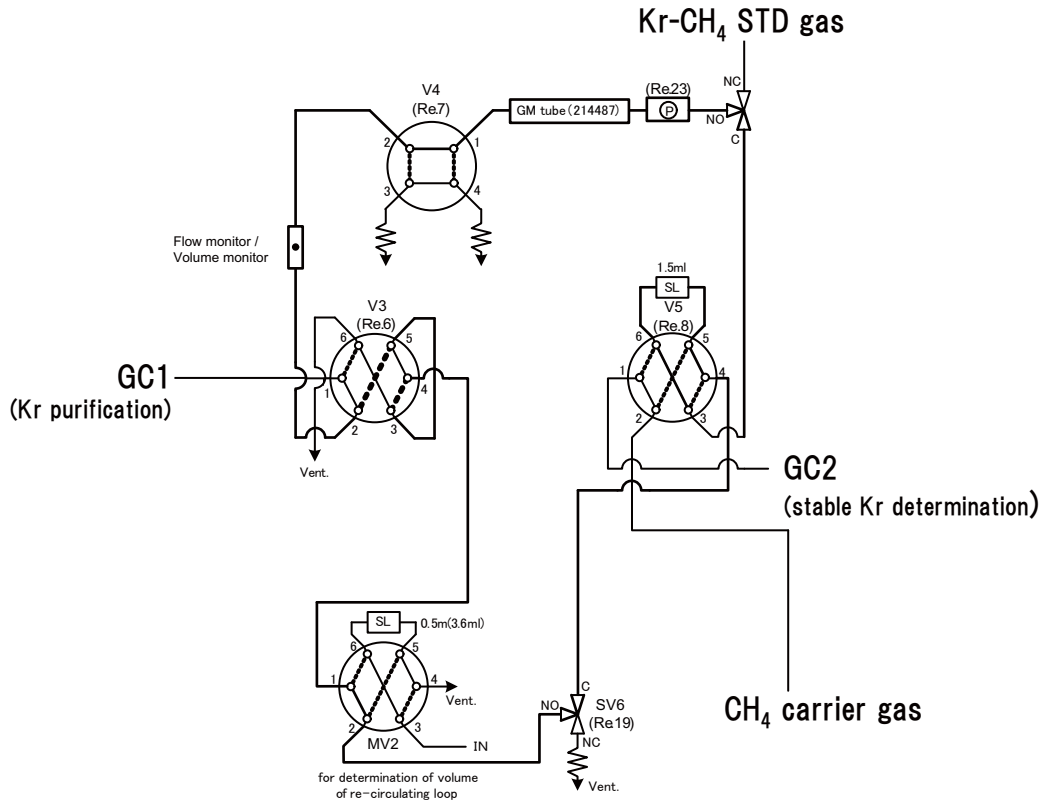

Figure 2.9 Schematic flow chart of recirculating loop

2.4.1 Operation of the proportional counter

Figure 2.10 depicts the plateau curve of the center proportional counter that is used for the ^{85}Kr activity measurement. For the measurement of the plateau curve Kr gas corresponding to 3% of the recirculating loop volume was introduced and mixed with CH_4. Since the Kr gas produced at present from air already contains ^{85}Kr, pure Kr gas itself is a good activity source. A counting time of 5 min was applied for each high-voltage value, giving the counting characteristics of the counter. The signal output began at 3400 V and a

plateau was attained between 3600 and 4000 V. Highly stable counting was achieved with the present proportional counter. Dependent on the counter plateau the high voltage for the ^{85}Kr measurement was set to a value between 3600 and 3800 V to optimize the counting performance. It should be noted that long use of proportional counters finally result in disappearance of the plateau. This ageing effect may be caused by the deposition of carbonaceous material on the surfaces of the detector arising from decomposition of the measurement gas, CH_4.

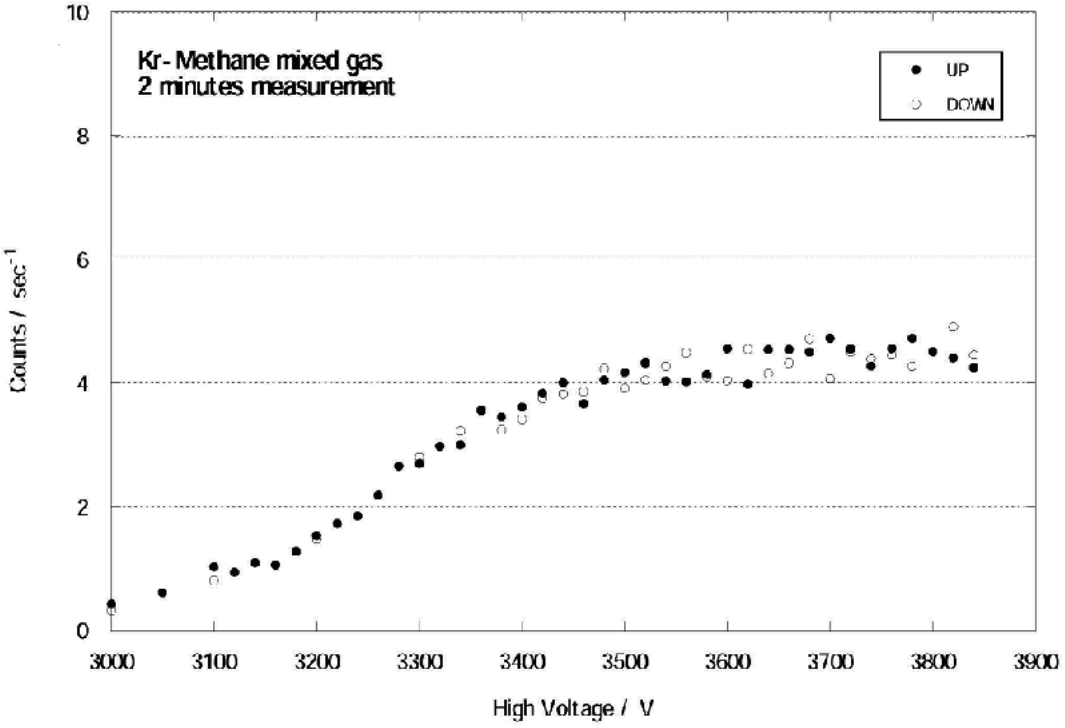

Figure 2.10 Plateau curve of the center proportional counter

Activity counting (u) gave a good linear response to the stable Kr volume (v) in the recirculating loop system (in one instance, u=24.84+31.39v, r~0.999, for 0.8-8.0 ml of stable Kr, n~5). This result indicated that the activity counting was not affected by a trivial change of gas composition in the proportional counter accompanied by varying Kr content.

Table 3 in Igarashi et al., (2001) gave the activity-counting efficiency of the proportional counter of the MRI system. It was obtained by using the reference Kr gas of which the ^{85}Kr activity was determined with the BfS system in Freiburg. Thus the MRI and the BfS systems had a common calibration regarding ^{85}Kr activity measurement. A counting efficiency of 55 to 60% was achieved with the present system. The data were in good accordance with the volume ratio of the proportional counter to the whole recirculating loop suggesting that the active volume of the proportional counter was 85 to 90%. Currently the proportional counter is shielded by 10 cm thick lead bricks and no other background reduction procedures have been applied. The background count rate for the proportional counter is 80 counts min^{-1}. However ^{85}Kr has a relatively high concentration level of at least 1 Bq m^{-3}, and it is fairly easy to measure ^{85}Kr activity with high precision. The current detection limit defined by 3.29 times one sigma of background is 0.02 Bq m^{-3} under the present conditions. Since the detection limit of the stable Kr measurement is of the order of some tens ppmv at the GC 3, the major factor controlling the detection limit of this system is the activity measurement rather than stable Kr measurement.

2.4.2 Anti-coincidence counting

We introduced an anti-coincidence technique to reduce the counting background. The anti-coincidence system consists of a center proportional counter and an outer proportional counter. The center proportional counter is inserted into the outer proportional counter (No. 49215, LND, USA) for anti-coincidence counting which is operated at a high voltage of 940 V using the counting gas, He 99.05% with 2-methyl-propane 0.95%. The high voltages for both proportional counters are supplied by a four channel HV power supply unit (RPH-012, Repic, Japan) and generated signals are amplified by preamplifier (Model

142AH, Ortec, USA). The signals from the preamplifier are sent to a discriminator unit (Model 705, Phillips Scientific, USA). The functions of this unit are to set the threshold level of the signal height and to convert the signal over the threshold level into digital signal. The signals are then sent to a gate-delay generator unit (Model 794, Phillips Scientific, USA). The functions of this unit are to delay the signal from the center proportional counter and to convert the signal from the outer proportional counter into a gate signal. Each signal is processed by logic units (Model 756&757, Phillips Scientific, USA) and an anti-coincidence circuit is built. The signals through the anti-coincidence circuit are output to a single channel analyzer (RPN-032, Repic, Japan) as counts. The activity-counting unit is presented in Fig. 2.11. Signal cable connections are depicted in Fig. 2.12. In the MRI system, the anti-coincidence technique reduces the background by a factor of 10 to 8 counts min^{-1}.

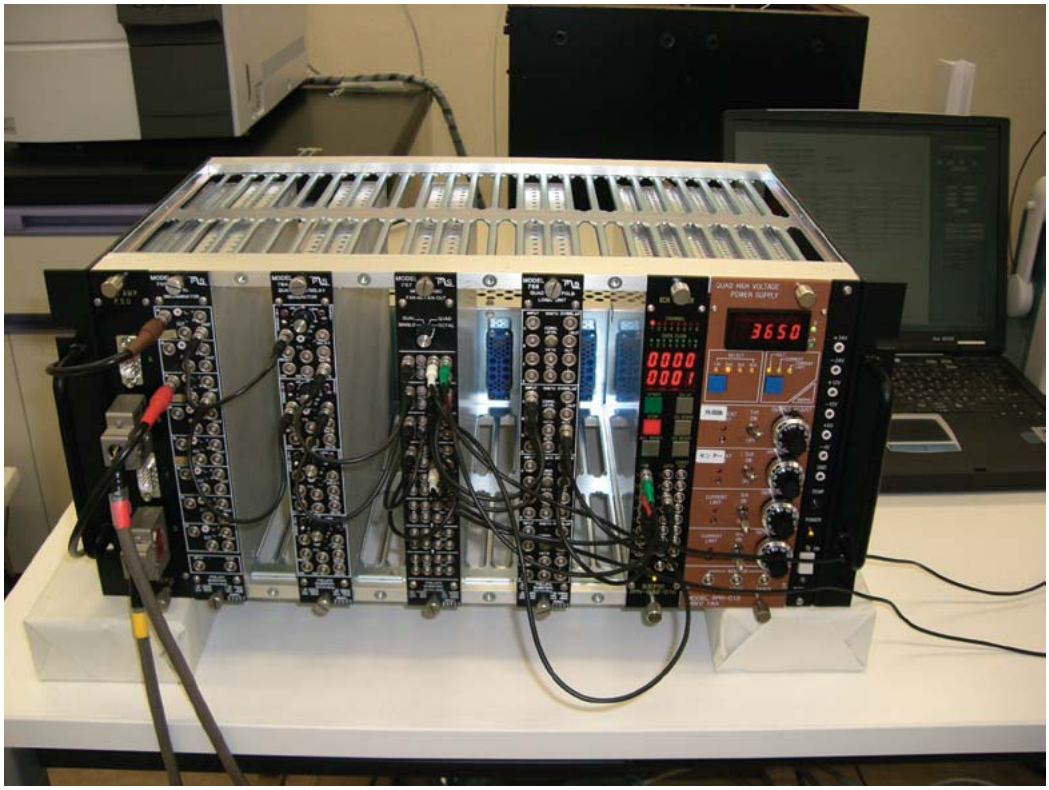

Figure 2.11 Activity counting unit (Electronics of the counting system)

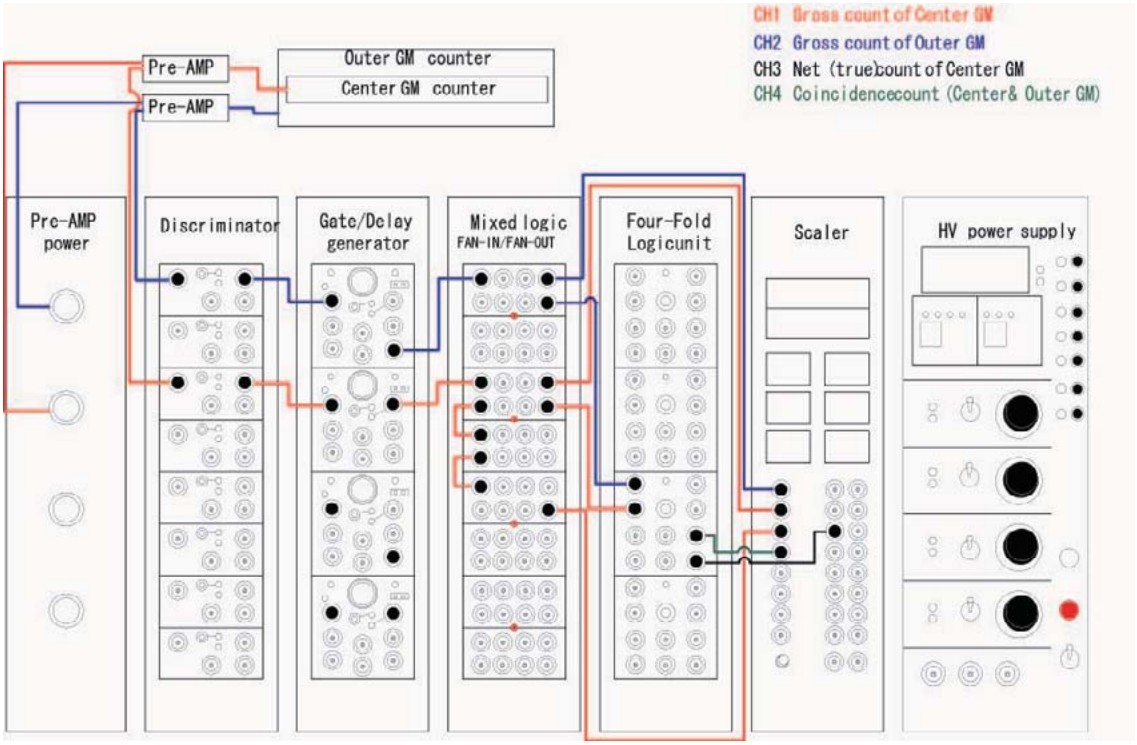

Figure 2.12 Diagram of signal cable connection

The ^{85}Kr measurement is continued until at least 10000 net counts have been obtained. Before and after the sample counting, background measurements are conducted to confirm the sample purge which replaces the sample gas by pure methane gas in the loop.

Along with the activity counting, the amount of stable Kr in the recirculating loop is precisely determined by GC3. Consequently the specific activity of ^{85}Kr (Bq ml^{-1}) is obtained from the activity measurement by the proportional counters and the amount of stable Kr is determined by a gas chromatograph.

2.5 Determination of the amount of stable Kr

The volume concentration of stable Kr in the loop is precisely determined by the gas

chromatograph (GC2014, Shimadzu, Japan). In this gas chromatograph (GC3) pure He gas is used as a carrier gas and its main column for separation is packed with MS-5A.

An example of a gas chromatogram is presented in Fig. 2.13. It is important to confirm that the peaks of krypton and methane are well-separated (not overlapped) in the gas chromatogram. When the separation of the main column is incomplete, the MS-5A column should be regenerated or exchanged. The presence of oxygen in the proportional counter reduces the activity count rate. Confirm that no peaks of air components (O_2 and N_2) are present in the gas chromatogram. If air peaks exists in the gas chromatogram, it is necessary to check the air tightness of each connection and six-ways valve. The Kr gas in the sample loop in re-circulation loop is subjected to analyze stable krypton concentration.

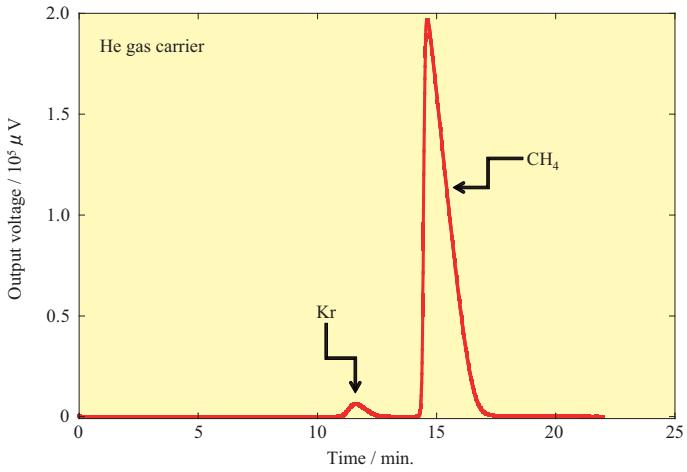

Figure 2.13 Chromatogram of stable Kr determination

In GC3 the gas in the sample loop (2 ml) is analyzed, after the loop is opened until its pressure becomes equilibrium with atmospheric pressure. The sample volume determined with GC3 depends on the temperature and air pressure, Therefore, analytical results obtained by the GC3 should be corrected to a standard condition for a fixed temperature (0

ºC) and air pressure (1 atm), which are monitored in the measurement room. The krypton volumes are corrected to standard temperature and pressure conditions (STP; 0 ºC, 1 atm). The Boyle-Charle's law is applied to the correction of the Kr volume assuming that the Kr gas behaves as an ideal gas.

Three gravimetric-made standard Kr-CH_4 mixed gases are used to calibrate GC3 prior to and after determine the stable Kr volume in the sample. The stable Kr volume concentrations in the standard gases using the calibration of the GC3 are determined, taking into account the Kr amount in the sample gas. The Kr volume concentrations in the three standard gases used are 0.5, 1 and 3 %.

2.6 Schedule of sample analysis

The time required for a sample analysis is as follows.

Calibration of the GC3 requires three hours before the sample analysis, but this calibration is performed automatically by a basic program. It takes one hour for the pre-treatment unit to separate the air components coarsely. It takes 30 minutes to separate and purify the Kr gas. Two to three hours are needed to measure the activity, depending on the Kr recovery and its activity level. It takes 30 minutes to determine the concentration of stable Kr in the sample. Nine hours are needed to carry out all analytical processes, including in a sample analyis. Therefore, only one sample can be analyzed per day in the current ^{85}Kr measurement system. The system operation for ^{85}Kr analysis is carried out as follows.

The pre-treatment unit is turned on just before the sample analysis and turned off after the sample analysis. However He gas continues to flow at a low flow rate in the pre-treatment unit to prevent moisture or other redundant components to attach to the

pre-treatment tube (Trap1). The GC1 and GC2 use methane gas as a carrier. In consideration of safety the GC1 and GC2 are turned on just before the sample analysis. After the sample analysis they are turned off and the carrier gas flow is also stopped. GC3 operates continuously to perform automatic calibration every morning. However, GC3 is turned off and the carrier gas flow is stopped on the weekend to control the consumption of He gas.

To ensure the ^{85}Kr measurement system operates normally a standard gas of a known ^{85}Kr activity concentration is analyzed once a week.

This schedule of sample analysis for a week is presented in table 2.1. Three samples can be analyzed in a week and if the GC3 is operated continuously during a weekend, starting of the system is unnecessary. Consequently four samples can be analyzed in a week.

Table 2.1 Schedule of sample analysis

Day of the week	Operation
Monday	System starting
Tuesday	Standard gas analysis
Wednesday	Sample analysis
Thursday	Sample analysis
Friday	Sample analysis

If the ^{85}Kr measurement system is shut down for a long time, the schedule is as follows.

For a comparatively short suspension (one week), He gas continues to flow at a rate of 10 ml min^{-1} through the pre-treatment unit (Trap1). GC3 is turned off and its carrier gas flow is also stopped. For a long suspension the flow of He gas through the pre-treatment unit is stopped, the power of this unit is shut down and all the valves are closed. The

proportional counter counting unit (e.g., PC and logic units) and other devices, such as the GC controller (Chromatopac C-R7A, Shimadzu, Japan), are also turned off. In the Kr enrichment tube (Trap2), a He gas flow continues at a small flow rate. In the proportional counter CH_4 gas continues to flow at a small flow rate or it should be formed a closed loop to avoid absorption of the air components and moisture to the proportional counter.

2.7. Calculation of atmospheric ^{85}Kr activiy concentration

The atmospheric ^{85}Kr activity concentration （Bq m^{-3}） is calculated by multiplying the abundance ratio of the stable Kr in the air (1.14 ml m^{-3}) by the specific activity (Bq ml^{-1}) obtained from the proportional counter activity measurement and the stable Kr determination by the gas chromatograph. It should be noted that the chemical recovery of Kr need not to be determined to obtain the atmospheric ^{85}Kr activity concentration, which is one of the characteristics of the method as developed by the BfS.

The activity concentration of atmospheric ^{85}Kr can be calculated by

$$\mathrm{A} = R_s \times \frac{1}{\mathrm{E}} \times \frac{1}{C_s \times V} \times M \qquad \cdots 2.1$$

where A is the activity concentration of atmospheric ^{85}Kr, R_s is the net count rate of the sample, E is the counting efficiency, C_s is the stable Kr concentration in the recirculating loop, V is the volume of the recirculating loop and M is the abundance ratio of stable Kr in the air.

From equation 2.1, it is necessary to determine the counting efficiency of the propotional

counter in advance to calculate the concentration of the atmospheric ^{85}Kr. There are two ways to determine the proportional counter counting efficiency. One is to determine the absolute efficiency for beta particles in the active area by evaluating precisely the non-active area. The other is to calculate the proportional counter counting efficiency by using a standard gas with well known ^{85}Kr activity concentration. The first method needs several kinds of the same type of proportional counters which have different active volumes with known length and diameter. The counting efficieny of the BfS system was dertermined applying this method. However this method is not easy, so the latter using the known concentration standard gas is adopted for the determination of the counting efficiency of the MRI system.

Using the known activity concentration of the standard gas the proportional counter counting efficiency can be found from the following equation:

$$\mathrm{E} = \frac{R_{std}}{S_{std} \times C_{std} \times V} \qquad \cdots 2.2$$

where R_{std} is the net count rate of the standard gas, S_{std} is the specific activity of the standard gas and C_{std} is the stable Kr concentration in the recirculating loop.

Equation 2.1 can be transformed into the following equation by substituting the proportional counter counting efficiency (E):

$$\mathrm{A} = \frac{R_s}{R_{std}} \times \frac{C_{std}}{C_s} \times S_{std} \times M \qquad \cdots 2.3$$

2.8 Uncertainty of atmospheric ^{85}Kr activity concentration

We consider two kinds of error terms: accuracy (systematic bias of the data) and precision (size of the randomness of the data). Accuracy is currently interpreted as traceability. The traceability of the data is ensured by using the Kr standard gas of which the ^{85}Kr activity was determined by the BfS. Therefore it is necessary to estimate the precision of the data separately and it is necessary to estimate the uncertainty involved in each measurement.

It is necessary to estimate the uncertainty of the proportional counter counting efficiency and the volume of the recirculationg loop using equation 2.1. However this equation can be transformed into equation 2.3 by using the mixed standard gas, which has a known activity concentration of ^{85}Kr. We therefore have to estimate only the uncertainty involved in the radioactivity measurement, in the stable Kr analysis and of the specific activity of the mixed standard gas for the determination of the uncertainty of the ^{85}Kr activity concentration.

a Radioactivity measurement

The uncertainty in the radioactivity measurement is estimated as the result of the counting error (square root of the count). Since a net counting rate is substituted for a background counting rate from a gross counting rate, the counting error must be calculated according to the four rules of arithmetic with error. The uncertainty in the radioactivity measurement is

$$\sigma_N = \sqrt{\left(N/t\right)^2 + \left(N_{B1} + N_{B2}/t_{B1} + t_{B2}\right)^2} \qquad \cdots 2.4$$

where σ_N is the uncertainty of the sample (σ_{Ns}) and the standard (σ_{Nstd}) in the radioactivity measurement, N is the gross count of the sample (N_s) and the standard (N_{std}), N_{B1} and N_{B2} are the gross counts of the backgrounds, t is the counting time of the sample (t_s) and the standard (t_{std}), and t_{B1} and t_{B2} are the counting times of the backgrounds.

b Stable Kr analysis

The stable Kr concentration in the recirculationg loop is determined by the working curve obtained by analyzing the standard gas which has a known concentration of the stable Kr. Therefore, the concentration of the stable Kr is calculated by the regression line

$$C = b \times E_0 + a \qquad \cdots 2.5$$

where C is the concentration (%) of stable Kr of the sample(C_s) and the standard(C_{std}) in the recirculationg loop. Here, E_0 is the accumulated thermal conductivity under standard conditions (0 ºC, 1atm) of the sample gas and the standard gas, a is the intercept, and b is the slope of linear regression.

The intercept and slope in this regression curve are included the uncertainty of the Kr standard gas analysis. This uncertainty spread to the stable Kr concentration in the sample. When the standard deviations of the intercept and slope are introduced as the uncertainty of the regression curve, the uncertainty in the stable Kr analysis is

$$\sigma_C = \sqrt{{\sigma_a}^2 + \left(E_0 \times \sigma_b\right)^2} \qquad \cdots 2.6$$

where σ_C is the uncertainty of the stable Kr analysis of the sample gas(σ_{Cs}) and the standard gas(σ_{Cstd}), σ_a and σ_b are the standard deviations of the intercept and slope.

The standard deviations of the intercept and slope in the regression curve are defined as

$$\sigma_a = \sigma_{y/x} \sqrt{\frac{\sum_i {x_i}^2}{n \sum_i \left(x_i - \bar{x}\right)^2}} \qquad \cdots 2.7$$

$$\sigma_b = \frac{\sigma_{y/x}}{\sqrt{\sum_i \left(x_i - \bar{x}\right)^2}} \qquad \cdots 2.8$$

$$\sigma_{y/x} = \left\{ \frac{\sum_i \left(y_i - \hat{y}_i\right)^2}{n-2} \right\}^{1/2} \qquad \cdots 2.9$$

where $\sigma_{y/x}$ is a statistical value that estimates the accidental error of the direction of a y-axis in the regression curve and is used for calculating the standard deviations of the intercept and the slope, x_i is the accumulated thermal conductivity in each analysis, $\bar{x}$ is the average of the accumulated thermal conductivity, n is the number of the data, y_i is the stable Kr concentration of the standard gas and $\hat{y}_i$ is the stable Kr concentration calculated by the working curve.

The mixed ^{85}Kr standard gas used to calibrate the ^{85}Kr measurement system was also

used to determine the proportional counter counting efficiency. The specific activity and the net counting rate of the mixed standard gas are necessary to determine the concentration of ^{85}Kr. Therefore the ^{85}Kr activity concentration needs not to be determined the proportional counter counting efficiency and the volume of the recirculationg loop from equation 2.7.3.

The specific activity determined by the BfS ($S_{std} \pm \sigma_{Sstd}$) is 0.9781 ± 0.004 Bq ml^{-1}.

We adopt this counting error as the uncertainty of the specific activity.

The uncertainty in the ^{85}Kr activity concentration can be estimated by the combination of uncertainties from each source. Before the combination, the uncertainties must be unified into relative standard uncertainty. By combining of the relative standard uncertainties from each source, the combined standard uncertainty (U_c) can be calculated as

$$U_C = \sqrt{\left(\sigma_{Ns}/N_s\right)^2 + \left(\sigma_{Nstd}/N_{std}\right)^2 + \left(\sigma_{Cstd}/C_{std}\right)^2 + \left(\sigma_{Cs}/C_s\right)^2 + \left(\sigma_{Sstd}/S_{std}\right)^2} \quad \cdots 2.10$$

An example of uncertainties from each source is shown in Table 2.2.

Table 2.2 Uncertainties involved in ^{85}Kr measurement

Sources	Relative standard uncertainty (%)
Radioactivity measurement (Terms1 and 2 in Eqn. 2.10)	1.5
Stable Kr analysis (Terms 3 and 4 in Eqn. 2.10)	0.5
Specific activity of the mixed standard gas (Term 5 in Eqn. 2-10)	0.5
Combined standard uncertainty (U_C, k=1)	1.7

2.9 New ^{85}Kr measurement system

The new ^{85}Kr measurement system of JCAC is constructed based on the system at MRI

along with the technical transfer of the ^{85}Kr monitoring system from MRI to JCAC. This new system consists of the sampling unit, the pre-treatment unit, the gas chromatographs for the purification of Kr (GC1) and for the determination of the amount of stable Kr (GC2) and the proportional counter. Three sampling units have been made in consideration of the framework of ^{85}Kr monitoring in JCAC.

The ^{85}Kr sampling unit is almost the same as the MRI sampling unit including the metal absorber. However the instrument for the preliminary removal of moisture has been modified from a remodeled refrigerator to a thermoelectric dehumidifier (DH-109, Komatsu Electronics Inc., Japan). The diagram of the sampling unit and the absorber are presented in Fig. 2.2 and Fig. 2.3, respectively.

The new ^{85}Kr measurement system has some improvements taking into consideration the framework of JCAC and the convenience of the usage, although the ^{85}Kr measurement system was also based on the MRI system. The improvements in the system of JCAC are as follows.

1) The number of the gas chromatographs has been changed from 3 to 2:
   In the framework of the environmental radioactivity monitoring at JCAC, the target noble gaseous radionuclide is ^{85}Kr only, so that the GC2 for purifying Xe was not considered.
2) In the pre-treatment unit has an additional He gas line for a pure water supply:
   The pure water in a water tank can be automatically filled into a water column by pressurizing He gas.
3) The connection of the cables for the activity measurement has been modified:
   The JCAC system uses two proportional counters simultaneously for sample

analysis. The delay method of the center proportional counter signal by the gate/delay generator is changed by passing through the Mixed Logic unit several times. The signal is delayed by physical processing. The connection of the cables among the units for the activity measurement of JCAC is illustrated in Fig. 2.12.

3. Standard gas for ^{85}Kr measurement

A simulated gas with a composition similar to that of the actual sample gas in the aluminum bottle (minican) is necessary to calibrate the ^{85}Kr measurement system and to fix its measurement conditions. In the early stages of development the major gas in the aluminum bottle was considered to be He and the simulated gas was prepared with the expected composition. However when the actual sample gas was analyzed, its composition differed from the expected one. Table 3.1 presents the actual sample gas compositions in the aluminum bottle along with those of the simulated gas (Takachiho Chemicals, Japan) based on this determination.

Table 3.1 Gas composition of the sample in the aluminum bottle and the simulated gas

Unit: (%)

Sample	He	Ar	N_2	O_2	Kr	CH_4	CO_2	Xe	Total
110-B	NA	NA	21.5	9.10	0.178	0.192	61.5	NA	92.5
178-B	10.4	NA	17.9	10.5	0.208	0.194	60.3	NA	99.5
179-B	6.89	NA	12.8	16.1	0.234	0.232	63.0	NA	99.3
Average	8.65	NA	17.4	11.9	0.207	0.206	61.6	NA	97.1
Simulated gas B	8.12	0.903	20.9	9.76	1.07	0.949	57.84	0.451	99.55

NA, not analyzed

This table is reproduced from Tabble 2 in Igarashi et al., 2001.

The result revealed that a major component of the sample gas in the aluminum bottle is CO_2 rather than He, N_2 and O_2. This result suggests that CO_2 has a high affinity to the activated charcoal. Therefore the major component in the simulated gas was changed from He to CO_2 (ca. 60%). As a result removal of CO_2 became a key point for the activity

measurement of ^{85}Kr. The CO_2 in the air contains both natural and anthropogenic ^{14}C and radio carbon interferes with the activity measurement of ^{85}Kr. The alkali-wet column, which can react more quickly with CO_2 in the sample, was therefore devised in the pre-treatment unit. Water is essential to complete the chemical reaction of CO_2 with alkaline agents. Although water is inadequate for gas chromatographic separation, a wet column was introduced for effective removal of a large amount of CO_2 (more than a few hundred milliliters).

Usually 4000 ml of the simulated gas was introduced into the system to adjust the whole ^{85}Kr measurement system. Therefore about 2400 ml of CO_2, about 800 ml of N_2 and about 400 ml of O_2 were injected into the pre-treatment unit along with about 40 ml of Kr.

4. Atmospheric ^{85}Kr in Japan

4.1 ^{85}Kr activity at Tsukuba since 1995

We had observed the weekly average atmospheric ^{85}Kr activity concentrations in ground level air in Tsukuba during the period from May 1995 to March 2006. Monthly averaged ^{85}Kr activity concentrations are shown in Table 4.1, and weekly atmospheric ^{85}Kr activity concentration are shown in Table 4.2, respectively. During the period that the nuclear fuel reprocessing plant at Tokai was in operation (before May 1997 and after June 2000), high ^{85}Kr activity concentrations exceeding 2 Bq m^{-3} were observed. On the other hand, low ^{85}Kr activity concentrations of less than 1.6 Bq m^{-3} were observed when operations at the Tokai plant were suspended. Compared with reprocessing plants in Europe, the magnitude of the emission at the Tokai plant is less than 10% of those in Europe (United Nations, 2000).

Table 4.1 Monthly averaged atmospheric ^{85}Kr activity concentrations in Tsukuba
Unit: Bq m^{-3}

	1995	1996	1997	1998	1999	2000	2001	2002	2003	2004	2005	2006
Jan		1.26	1.26	1.3	1.37	1.35	1.36	1.46	1.45	1.89	1.50	1.50
Feb		1.24	3.34	1.31	1.36	1.37	1.34	1.47	1.43	1.94	2.43	3.94
Mar		1.23	1.29	1.29	1.37	1.36	1.92	1.55	1.44	1.78	4.80	1.52
Apr		2.44	1.27	1.27	1.37	1.38	3.13	3.88	1.45	1.99	2.82	
May	6.88	4.35	1.31	1.29	1.36	1.32	2.48	4.86	1.49	2.55	2.76	
Jun	2.11	2.29	1.26	1.25	1.32	1.33	2.85	3.50	1.44	1.45	1.45	
Jul	1.08	1.16	1.23	1.21	1.25	2.02	1.29	1.30	1.41	1.40	1.44	
Aug	1.06	1.16	1.19	1.21	1.24	1.25	1.33	1.32	1.36	1.43	1.40	
Sep	5.3	1.99	1.23	1.22	1.3	1.3	1.39	1.37	2.40	1.45	1.40	
Oct	4.29	5.03	1.27	1.32	1.39	1.37	3.18	2.09	3.55	4.92	2.80	
Nov	1.76	2.2	1.33	1.35	1.37	1.46	1.85	1.69	2.54	2.08	2.41	
Dec	1.33	1.23	1.36	1.4	1.41	1.39	1.51	1.50	1.47	1.54	1.53	

note: Monthly averaged atmospheric ^{85}Kr activity concentrations during the period from 1995 to 2001 are cited from Hirota et al., 2004.

Figure 4.1 plotts the atmospheric ^{85}Kr activity concentrations in Tsukuba observed from May 1995 to March 2006. Sporadic high ^{85}Kr activity concentrations were due to the effect of the release of ^{85}Kr from a nuclear fuel reprocessing plant at Tokai operated by Japan Nuclear Cycle Development Institute (JNC), 60 km northeast from the MRI (Igarashi et al., 2000).

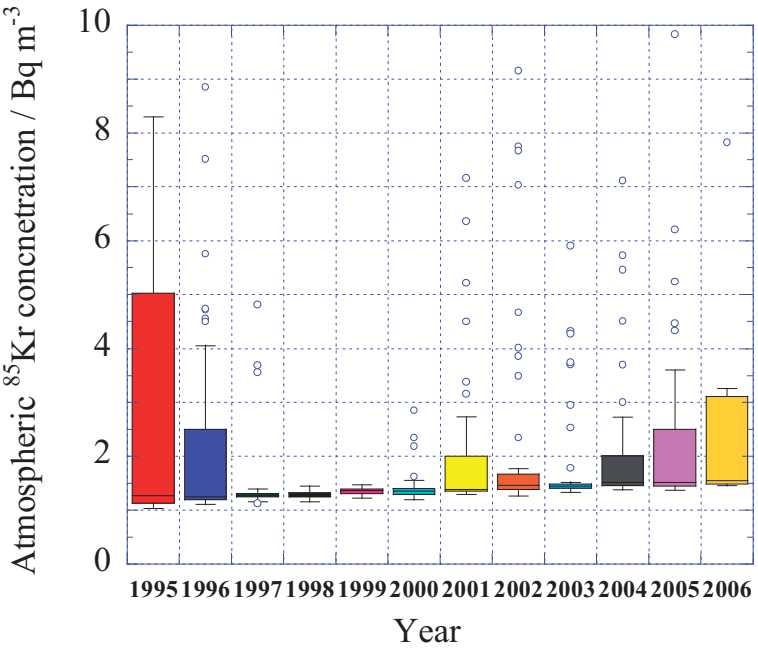

Figure 4.1 Atmospheric ^{85}Kr activity concentrations in Tsukuba observed from 1995 to 2006. Each box encloses 50% of the data with the median value of the variable displayed as a line. The top and bottom of the box mark the limits of +-25% of the variable population. The lines extending from the top and bottom of each box mark the minimum and maximum values within the data set that fall within an acceptable range. Any value out side of this range, called an outliter, is displayed as an individual plot. The acceptable range is defined as follows;
Upper quartile (UQ): The data value located halfway between the median and the largest data value.
Lower quartile (LQ): The data value located halfway between the median and the smallest data value.
Outliters-Points whose data value is either:
greater than UQ + 1.5 x (UQ – LQ) or less than LQ – 1.5 x (UQ – LQ)

Because of a fire and explosion accident in March 1997 (STA, 1997, NSC, 1997, Igarashi et al., 1999), the operation of the nuclear fuel reprocessing plant at Tokai was

discontinued until the summer of 2000. During this period, no sporadic high ^{85}Kr activity concentrations in surface air were observed in Tsukuba. Experimental operation of the nuclear fuel reprocessing plant in Tokai was conducted in the summer of 2000, and its routine operation was restarted in the spring of 2001. Since that time, sporadic increases of atmospheric ^{85}Kr activity concentrations have occurred again in Tsukuba. For the public's radiation protection, it is important to know the background level of the atmospheric ^{85}Kr activity concentrations in Japan. For the background level of atmospheric ^{85}Kr activity concentrations in Tsukuba, data affected by ^{85}Kr release from the Tokai plant should be removed. Since the effect of ^{85}Kr release from the Tokai plant toto the atmosphere in Tsukuba depends on wind direction, wind speed, and daily ^{85}Kr release rate from the Tokai plant (Igarashi et al., 2000), all of the observed data in the sampling period including the days when the Tokai plant has been in operation were removed regardless of the ^{85}Kr activity concentration measured at MRI. The background data obtained are plotted in Fig. 4.2

The background atmospheric ^{85}Kr activity concentrations in Tsukuba have been increasing, accompanied by seasonal variations throughout our study period. Hirota et al. (2004) had showed that annual growth rate from 1996 to 2001 in Tsukuba was calculated to be 0.03 Bq m^{-3} yr^{-1}. This rate was at the same level as a previous estimate for the period of 1996 - 1998 (Igarashi et al. 2000). During the period from 1995 to 2006, the linear regression of atmospheric ^{85}Kr activity concentration also showed similar increasing rate of 0.03 Bq m^{-3} yr^{-1}. However, it must be noted that the growth rate varied annually, especially atmospheric ^{85}Kr activity concentration are almost constant since 2004. The mean annual growth rate of 0.03 Bq m^{-3} $yr^{-1}$is independently observed at all other stations of the global BfS noble gas network. The background values measured at the sites on the

Northern Hemisphere of the global BfS network are in good agreement with the one measured during winter time at MRI in Tsukuba. Pollard et al. (1997) reported the atmospheric ^{85}Kr activity concentrations at Clonskeagh, Dublin, Ireland, between 1994 and 1996. Excluding the data exceeding 2.5 Bq m^{-3} as outliers, the mean annual ^{85}Kr activity concentration was 1.12 Bq m^{-3} during 1994 and 1.30 Bq m^{-3} during 1996, and an increasing trend of approximately 0.1 Bq m^{-3} yr^{-1} was observed which is app. a factor of 3 higher than the ones measured at other sites in Europe and Japan. The atmospheric ^{85}Kr activity concentrations in Dublin from 1994 to1996 were in agreement with those observed in winter at the MRI, Tsukuba.

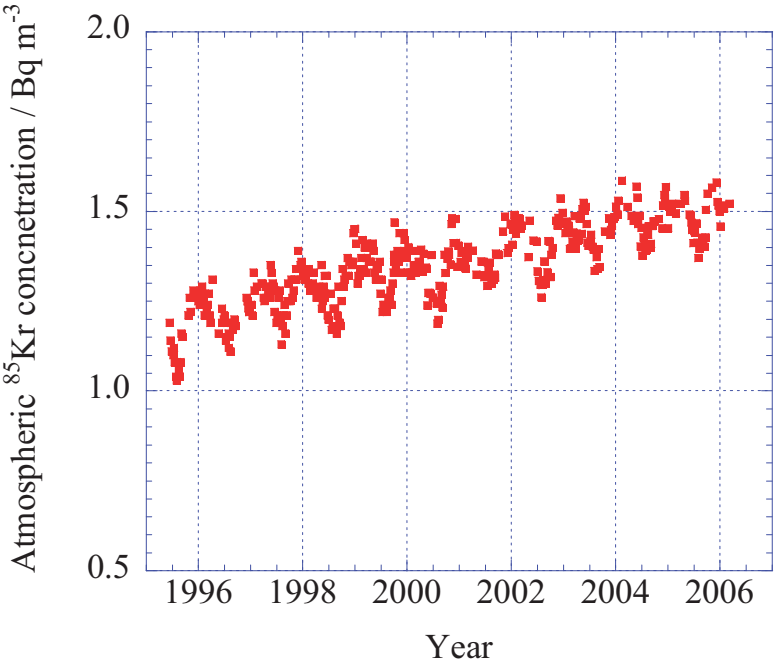

Figure 4.2 Atmospheric background ^{85}Kr activity concentrations in Tsukuba

The background atmospheric ^{85}Kr activity concentrations in Japan indicated a clear seasonal variation which is characterized as low in summer and high in winter. To explain this pattern of seasonal variation Hirota et al., (2004) had carried out the backward

trajectory analysis by using ^{85}Kr data observed in Tsukuba in 1999. They used Global Analysis Data (GANAL) compiled by the Japan Meteorological Agency for wind data analysis. A total of 240 hours backward data (starting at an altitude of 1,500 m, about 850 hPa; 00 UTC) was calculated every 5 days. Figure 4.3(a) illustrates typical examples of the backward trajectory in winter and Figure 4.3(b) depicts those, respectively.

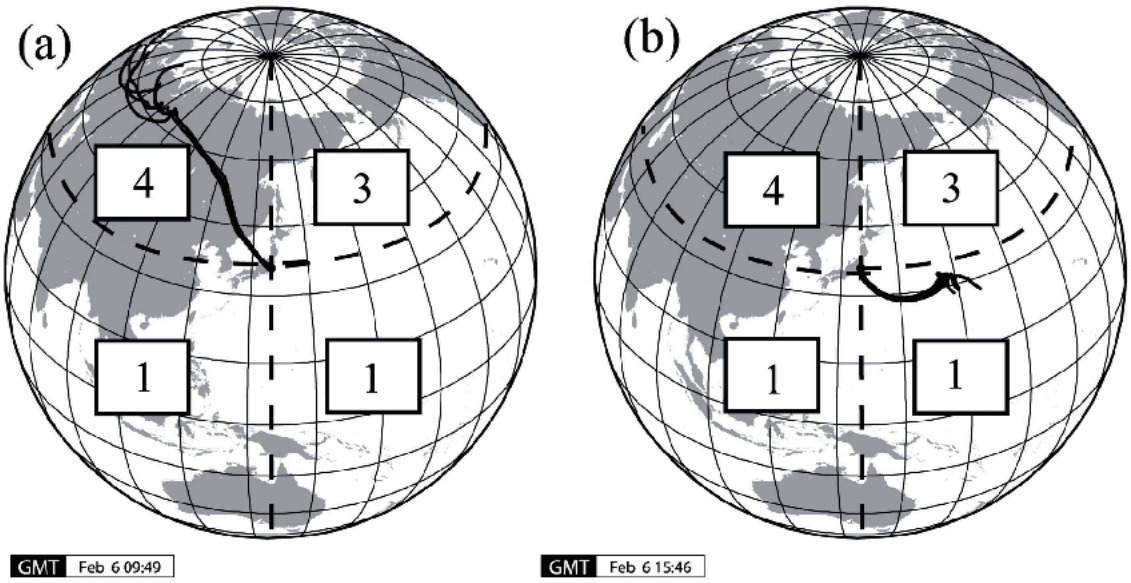

Figure 4.3 Typical charts of backward trajectory in winter and in summer. The point for each category is shown on the globe. (a) the chart for 10 days from January 5, 1999. (b) the chart for 10 days from August 3, 1999. (Hirota et al, 2004, figure 5)

In their analysis the origin of air mass transported to Tsukuba was estimated. The origins were grouped by four categories centering on Tsukuba, and they introduced the "Trajectory Index" of air masses to reflect the relative distribution of the global atmospheric ^{85}Kr activity concentrations. This index is defined as a mean of the points during the sampling period, in which the point on each day is assigned from the category of the trajectory (Figure 4.3). Since most of the nuclear fuel reprocessing plants are located in Europe, it is considered that the area classified as category 1 shows the highest concentrations of ^{85}Kr, i.e., the highest point. The areas classified as categories 3 and 4

show the lowest concentrations of ^{85}Kr, i.e., the lowest point. This classification reflects a latitudinal gradient of the atmospheric ^{85}Kr activity concentrations, high in the northern air mass and low in the southern air mass, which is in agreement with the observations reported by Weiss et al. (1992). We examined the correlation between the "Trajectory Index" and the observed atmospheric ^{85}Kr activity concentrations and found a good correlation between them (correlation factor 0.67) was found. Using a linear regression obtained from this correlation, we estimated ^{85}Kr activity concentrations in Tsukuba from the indexes. Figure 4.4 shows the comparison between the observed ^{85}Kr activity concentrations and the estimated ones from the indexes in Tsukuba. The result suggests that the seasonal variation of the atmospheric ^{85}Kr activity concentrations in Tsukuba, Japan, is mainly controlled by the transport of the air masses with different origins and that the high concentrations from October to May are attributable to the transport of the continental air mass directly affected by the European sources.

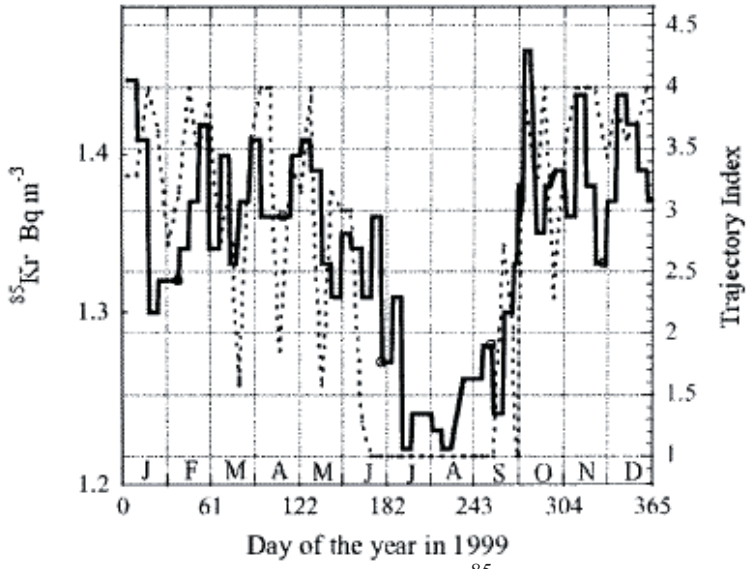

Figure 4.4 Comparison between the observed ^{85}Kr activity concentrations and the estimated ones from the "Trajectory Indexes" in Tsukuba in 1999. (Hirota et al., 2004 Figure 6)

Table 4.2 Weekly atmospheric ^{85}Kr activity concentration at Tsukuba during the period from May 1995 to March 2006.

code	start	stop	Duration day	^{85}Kr Bq m^{-3}	remark
BfS	1995.5.1	1995.5.8	7	7.67 ± 0.06	
BfS	1995.5.1	1995.5.8	7	7.78 ± 0.02	
BfS	1995.5.1	1995.5.8	7	7.72 ± 0.23	*
BfS	1995.5.8	1995.5.15	7	14.20 ± 0.06	
BfS	1995.5.15	1995.5.22	7	3.28 ± 0.03	
BfS	1995.5.22	1995.5.29	7	6.02 ± 0.03	
BfS	1995.5.29	1995.6.5	6	3.16 ± 0.03	
BfS	1995.6.5	1995.6.12	7	5.03 ± 0.05	
BfS	1995.6.5	1995.6.12	7	5.05 ± 0.05	
BfS	1995.6.5	1995.6.12	7	4.98 ± 0.03	
BfS	1995.6.5	1995.6.12	7	5.02 ± 0.15	*
BfS	1995.6.12	1995.6.19	6	1.19 ± 0.04	
BfS	1995.6.12	1995.6.19	6	1.19 ± 0.01	
BfS	1995.6.12	1995.6.19	6	1.19 ± 0.01	*
BfS	1995.6.19	1995.6.26	7	1.14 ± 0.01	
BfS	1995.6.26	1995.7.3	7	1.11 ± 0.01	
	1995.7.3		7	N.A	**
BfS	1995.7.10	1995.7.14	4	1.10 ± 0.01	
BfS	1995.7.14	1995.7.18	3	1.12 ± 0.01	
BfS	1995.7.18	1995.7.28	6	1.08 ± 0.01	
	1995.7.24		4		**
BfS	1995.7.28	1995.8.1	3	1.04 ± 0.01	
BfS	1995.8.1	1995.8.7	6	1.03 ± 0.01	
BfS	1995.8.7	1995.8.14	5	1.08 ± 0.01	
BfS	1995.8.14	1995.8.21	7	1.06 ± 0.01	
BfS	1995.8.21	1995.8.28	4	1.04 ± 0.01	
BfS	1995.8.28	1995.9.4	7	1.08 ± 0.01	
BfS	1995.9.4	1995.9.11	7	1.16 ± 0.01	
BfS	1995.9.11	1995.9.18	7	1.15 ± 0.00	
	1995.9.18		7	N.A	**
BfS	1995.9.25	1995.9.25	5	13.60 ± 0.10	
BfS	1995.9.25	1995.10.9	5	3.60 ± 0.05	
BfS	1995.10.9	1995.10.16	7	6.39 ± 0.03	
BfS	1995.10.16	1995.10.23	4	8.30 ± 0.03	
BfS	1995.10.23	1995.10.30	7	1.21 ± 0.01	
BfS	1995.10.30	1995.11.6	7	1.26 ± 0.01	
BfS	1995.11.6	1995.11.13	7	1.22 ± 0.01	
BfS	1995.11.13	1995.11.20	7	3.11 ± 0.02	
BfS	1995.11.20	1995.11.27	7	1.41 ± 0.01	
BfS	1995.11.27	1995.12.4	7	1.28 ± 0.01	
BfS	1995.12.4	1995.12.11	7	1.27 ± 0.01	
BfS	1995.12.11	1995.12.18	7	1.42 ± 0.00	

Table 4.2 Continued

code	start	stop	Duration day	^{85}Kr Bq m^{-3}	remark
BfS	1995.12.18	1995.12.25	7	1.38 ± 0.01	
BfS	1995.12.25	1996.1.1	7	1.26 ± 0.00	
BfS	1996.1.1	1996.1.8	7	1.25 ± 0.00	
BfS	1996.1.8	1996.1.15	7	1.24 ± 0.01	
BfS	1996.1.15	1996.1.22	7	1.24 ± 0.01	
BfS	1996.1.22	1996.1.29	7	1.28 ± 0.01	
BfS	1996.1.29	1996.2.5	7	1.29 ± 0.01	
BfS	1996.2.5	1996.2.12	7	1.25 ± 0.01	
BfS	1996.2.12	1996.2.19	7	1.21 ± 0.01	
BfS	1996.2.19	1996.2.26	7	1.27 ± 0.01	
BfS	1996.2.26	1996.3.5	7	1.23 ± 0.01	
BfS	1996.3.5	1996.3.12	6	1.24 ± 0.01	
BfS	1996.3.12	1996.3.19	6	1.27 ± 0.01	
BfS	1996.3.19	1996.3.25	6	1.21 ± 0.01	
BfS	1996.3.25	1996.4.2	7	1.19 ± 0.01	
BfS	1996.4.2	1996.4.9	6	1.81 ± 0.02	
BfS	1996.4.9	1996.4.16	6	1.31 ± 0.01	
BfS	1996.4.16	1996.4.23	6	4.55 ± 0.02	
BfS	1996.4.23	1996.4.30	6	2.93 ± 0.02	
BfS	1996.4.30	1996.5.7	6	1.61 ± 0.01	
BfS	1996.5.7	1996.5.14	6	7.52 ± 0.05	
BfS	1996.5.14	1996.5.21	6	5.76 ± 0.03	
BfS	1996.5.21	1996.5.28	6	1.16 ± 0.01	
BfS	1996.5.28	1996.6.4	6	2.95 ± 0.01	
BfS	1996.6.4	1996.6.10	6	3.11 ± 0.02	
BfS	1996.6.10	1996.6.14	4	4.72 ± 0.04	
BfS	1996.6.14	1996.6.17	3	1.23 ± 0.01	
BfS	1996.6.17	1996.6.24	7	1.19 ± 0.01	
BfS	1996.6.24	1996.7.1	7	1.20 ± 0.00	
BfS	1996.7.1	1996.7.8	7	1.21 ± 0.01	
BfS	1996.7.8	1996.7.15	7	1.14 ± 0.01	
BfS	1996.7.15	1996.7.22	7	1.15 ± 0.00	
BfS	1996.7.22	1996.7.30	7	1.19 ± 0.01	
BfS	1996.7.30	1996.8.1	2	1.12 ± 0.01	
BfS	1996.8.1	1996.8.5	4	1.16 ± 0.01	
BfS	1996.85	1996.8.12	7	1.15 ± 0.01	
BfS	1996.8.12	1996.8.19	7	1.11 ± 0.01	
BfS	1996.8.19	1996.8.26	7	1.19 ± 0.01	
BfS	1996.8.26	1996.9.2	7	1.17 ± 0.01	
BfS	1996.9.2	1996.9.9	7	1.18 ± 0.01	
BfS	1996.9.9	1996.9.16	7	1.20 ± 0.01	
BfS	1996.9.16	1996.9.23	7	1.18 ± 0.01	
BfS	1996.9.23	1996.9.30	7	1.64 ± 0.01	
BfS	1996.9.30	1996.10.7	4	4.74 ± 0.03	

Table 4.2 Continued

code	start	stop	Duration day	^{85}Kr Bq m^{-3}	remark
BfS	1996.10.7	1996.10.15	7	8.85 ± 0.05	
BfS	1996.10.15	1996.10.21	3	4.50 ± 0.04	
BfS	1996.10.21	1996.10.28	7	2.72 ± 0.01	
BfS	1996.10.28	1996.11.5	7	4.05 ± 0.02	
BfS	1996.11.5	1996.11.11	6	3.09 ± 0.02	
BfS	1996.11.11	1996.11.18	7	1.65 ± 0.04	
BfS	1996.11.18	1996.11.25	7	2.50 ± 0.01	
BfS	1996.11.25	1996.12.2	7	1.56 ± 0.01	
BfS	1996.12.2	1996.12.9	7	1.26 ± 0.01	
BfS	1996.12.9	1996.12.16	7	1.25 ± 0.01	
BfS	1996.12.16	1996.12.23	7	1.23 ± 0.01	
BfS	1996.12.23	1996.12.25	2	1.22 ± 0.02	
BfS	1996.12.25	1997.1.6	2	1.22 ± 0.00	
BfS	1997.1.6	1997.1.13	7	1.24 ± 0.01	
BfS	1997.1.13	1997.1.20	7	1.21 ± 0.01	
BfS	1997.1.20	1997.1.27	7	1.33 ± 0.01	
BfS	1997.1.27	1997.2.3	7	1.28 ± 0.01	
BfS	1997.2.3	1997.2.10	7	4.82 ± 0.02	
BfS	1997.2.10	1997.2.17	7	3.69 ± 0.02	
BfS	1997.2.17	1997.2.24	4	1.29 ± 0.01	
BfS	1997.2.24	1997.3.3	7	3.56 ± 0.04	
			7	N.A	
			7	N.A	
			5	N.A	
BfS	1997.3.15	1997.3.17	2	1.30 ± 0.01	
BfS	1997.3.17	1997.3.24	7	1.30 ± 0.01	
BfS	1997.3.24	1997.3.31	7	1.30 ± 0.01	
BfS	1997.3.31	1997.4.7	7	1.26 ± 0.01	
BfS	1997.4.7	1997.4.14	7	1.25 ± 0.01	
BfS	1997.4.14	1997.4.21	7	1.29 ± 0.01	
BfS	1997.4.21	1997.4.28	7	1.26 ± 0.01	
BfS	1997.4.28	1997.5.5	7	1.29 ± 0.01	
BfS	1997.5.5	1997.5.12	7	1.28 ± 0.01	
BfS	1997.5.12	1997.5.19	7	1.26 ± 0.01	
BfS	1997.5.19	1997.5.26	7	1.35 ± 0.01	
BfS	1997.5.26	1997.6.3	7	1.33 ± 0.01	
BfS	1997.6.3	1997.6.9	6	1.30 ± 0.01	
BfS	1997.6.9	1997.6.16	7	1.29 ± 0.01	
BfS	1997.6.16	1997.6.23	7	1.22 ± 0.01	
BfS	1997.6.23	1997.6.30	7	1.28 ± 0.01	
BfS	1997.6.30	1997.7.7	7	1.19 ± 0.01	
BfS	1997.7.7	1997.7.14	7	1.21 ± 0.01	
BfS	1997.7.14	1997.7.21	7	1.26 ± 0.01	
BfS	1997.7.21	1997.7.28	7	1.28 ± 0.01	
BfS	1997.7.28	1997.8.4	7	1.19 ± 0.01	

Table 4.2 Continued

code	start	stop	Duration day	^{85}Kr Bq m^{-3}	remark
BfS	1997.8.4	1997.8.11	4	1.13 ± 0.01	
BfS	1997.8.11	1997.8.18	7	1.18 ± 0.01	
BfS	1997.8.18	1997.8.25	7	1.21 ± 0.01	
BfS	1997.8.25	1997.9.1	7	1.24 ± 0.01	
BfS	1997.9.1	1997.9.8	7	1.16 ± 0.01	
BfS	1997.9.8	1997.9.16	4	1.21 ± 0.01	
BfS	1997.9.16	1997.9.22	6	1.25 ± 0.01	
BfS	1997.9.22	1997.9.29	7	1.30 ± 0.02	
BfS	1997.9.29	1997.10.6	4	1.25 ± 0.01	
BfS	1997.10.6	1997.10.13	3	1.25 ± 0.01	
BfS	1997.10.13	1997.10.20	4	1.31 ± 0.01	
BfS	1997.10.20	1997.10.27	7	1.26 ± 0.01	
BfS	1997.10.27	1997.11.4	6	1.28 ± 0.01	
BfS	1997.11.4	1997.11.10	6	1.31 ± 0.01	
BfS	1997.11.10	1997.11.17	7	1.31 ± 0.01	
BfS	1997.11.17	1997.11.25	4	1.34 ± 0.01	
BfS	1997.11.25	1997.12.1	6	1.34 ± 0.01	
BfS	1997.12.1	1997.12.8	7	1.39 ± 0.01	
BfS	1997.12.8	1997.12.15	7	1.34 ± 0.01	
BfS	1997.12.15	1997.12.22	7	1.35 ± 0.01	
BfS	1997.12.22	1998.1.5	7	1.36 ± 0.01	
BfS	1998.1.5	1998.1.13	6	1.32 ± 0.01	
BfS	1998.1.13	1998.1.19	6	1.31 ± 0.01	
BfS	1998.1.19	1998.1.26	7	1.32 ± 0.01	
BfS	1998.1.26	1998.2.2	7	1.34 ± 0.01	
BfS	1998.2.2	1998.2.9	7	1.33 ± 0.01	
BfS	1998.2.9	1998.2.16	7	1.30 ± 0.01	
BfS	1998.2.16	1998.2.23	7	1.34 ± 0.01	
BfS	1998.2.23	1998.3.2	7	1.28 ± 0.01	
BfS	1998.3.2	1998.3.9	7	1.29 ± 0.01	
BfS	1998.3.9	1998.3.16	7	1.30 ± 0.01	
BfS	1998.3.16	1998.3.23	7	1.33 ± 0.01	
BfS	1998.3.23	1998.3.30	7	1.28 ± 0.01	
BfS	1998.3.30	1998.4.6	7	1.28 ± 0.01	
BfS	1998.4.6	1998.4.13	7	1.26 ± 0.01	
BfS	1998.4.13	1998.4.20	7	1.28 ± 0.01	
BfS	1998.4.20	1998.4.27	7	1.26 ± 0.01	
BfS	1998.4.27	1998.5.6	5	1.29 ± 0.01	
BfS	1998.5.6	1998.5.11	5	1.27 ± 0.01	
BfS	1998.5.11	1998.5.14	7	1.35 ± 0.01	
BfS	1998.5.14	1998.5.18	5	1.23 ± 0.01	
BfS	1998.5.18	1998.5.25	7	1.25 ± 0.01	
BfS	1998.5.25	1998.6.1	7	1.29 ± 0.01	
BfS	1998.6.1	1998.6.2	7	1.26 ± 0.01	
BfS	1998.6.2	1998.6.8	3	1.32 ± 0.01	

Table 4.2 Continued

code	start	stop	Duration day	^{85}Kr Bq m^{-3}	remark
BfS	1998.6.8	1998.615	7	1.27 ±0.01	
BfS	1998.6.15	1998.6.22	7	1.32 ±0.01	
BfS	1998.6.22	1998.6.29	7	1.21 ±0.01	
BfS	1998.6.29	1998.7.6	7	1.20 ±0.01	
			7	N.A	
BfS	1998.7.13	1998.7.21	4	1.27 ± 0.00	
BfS	1998.7.21	1998.7.29	8	1.17 ± 0.01	
BfS	1998.7.29	1998.8.3	5	1.18 ± 0.01	
BfS	1998.8.3	1998.8.10	7	1.23 ± 0.01	
BfS	1998.8.10	1998.8.17	7	1.23 ± 0.01	
BfS	1998.8.17	1998.8.24	7	1.23 ± 0.01	
BfS	1998.8.24	1998.8.31	7	1.16 ± 0.01	
BfS	1998.8.31	1998.9.7	7	1.21 ± 0.01	
BfS	1998.9.7	1998.9.14	7	1.29 ± 0.01	
BfS	1998.9.14	1998.9.21	7	1.19 ± 0.01	
BfS	1998.9.21	1998.9.28	7	1.18 ± 0.01	
BfS	1998.9.28	1998.10.5	7	1.25 ± 0.01	
BfS	1998.10.5	1998.10.12	5	1.34 ± 0.01	
BfS	1998.10.12	1998.10.19	7	1.29 ± 0.01	
BfS	1998.10.19	1998.10.26	4	1.31 ± 0.01	
BfS	1998.10.26	1998.11.3	7	1.32 ± 0.01	
			7	N.A	
BfS	1998.11.9	1998.11.16	7	1.37 ± 0.01	
BfS	1998.11.16	1998.11.23	7	1.32 ± 0.01	
BfS	1998.11.23	1998.11.30	7	1.36 ± 0.01	
BfS	1998.11.30	1998.12.7	7	1.36 ± 0.01	
BfS	1998.12.7	1998.12.14	7	1.35 ± 0.01	
BfS	1998.12.14	1998.12.21	7	1.36 ± 0.01	
BfS	1998.12.21	1998.12.28	7	1.44 ± 0.01	
BfS	1998.12.28	1999.1.4	7	1.45 ± 0.00	
BfS	1999.1.4	1999.1.11	7	1.45 ± 0.01	
BfS	1999.1.11	1999.1.18	7	1.41 ± 0.01	
BfS	1999.1.18	1999.1.25	7	1.30 ± 0.01	
BfS	1999.1.25	1999.2.1	7	1.32 ± 0.01	
BfS	1999.2.1	1999.2.8	7	1.32 ± 0.01	
BfS	1999.2.8	1999.2.15	7	1.34 ± 0.01	
BfS	1999.2.15	1999.2.22	7	1.37 ± 0.01	
BfS	1999.2.22	1999.3.1	7	1.42 ± 0.01	
BfS	1999.3.1	1999.3.8	7	1.34 ± 0.01	
BfS	1999.3.8	1999.3.15	7	1.40 ± 0.01	
BfS	1999.3.15	1999.3.23	5	1.33 ± 0.01	
BfS	1999.3.23	1999.3.29	6	1.37 ± 0.01	
BfS	1999.3.29	1999.4.5	7	1.41 ± 0.01	
BfS	1999.4.5	1999.4.12	7	1.36 ± 0.01	
BfS	1999.4.12	1999.4.19	7	1.36 ± 0.01	

Table 4.2 Continued

code	start	stop	Duration day	^{85}Kr Bq m^{-3}	remark
BfS	1999.4.19	1999.4.26	7	1.36 ± 0.01	
BfS	1999.4.26	1999.5.3	7	1.40 ± 0.01	
BfS	1999.5.3	1999.5.10	7	1.41 ± 0.01	
BfS	1999.5.10	1999.5.17	7	1.39 ± 0.01	
BfS	1999.5.17	1999.5.24	7	1.33 ± 0.02	
BfS	1999.5.24	1999.5.31	7	1.31 ± 0.01	
BfS	1999.5.31	1999.6.7	7	1.35 ± 0.01	
BfS	1999.6.7	1999.6.14	7	1.34 ± 0.01	
BfS	1999.6.14	1999.6.21	7	1.31 ± 0.01	
BfS	1999.6.21	1999.6.28	7	1.36 ± 0.01	
BfS	1999.6.28	1999.7.5	7	1.27 ± 0.01	
BfS	1999.7.5	1999.7.12	7	1.31 ± 0.01	
BfS	1999.7.12	1999.7.19	7	1.22 ± 0.01	
BfS	1999.7.19	1999.7.26	7	1.24 ± 0.01	
BfS	1999.7.26	1999.8.2	7	1.24 ± 0.01	
BfS	1999.8.2	1999.8.9	7	1.23 ± 0.01	
BfS	1999.8.9	1999.8.16	7	1.22 ± 0.01	
			7	N.A	
BfS	1999.8.23	1999.8.30	7	1.26 ± 0.01	
BfS	1999.8.30	1999.9.6	7	1.26 ± 0.01	
BfS	1999.9.6	1999.9.13	7	1.28 ± 0.00	
BfS	1999.9.13	1999.9.20	7	1.24 ± 0.01	
BfS	1999.9.20	1999.9.27	7	1.30 ± 0.02	
BfS	1999.9.27	1999.9.30	3	1.33 ± 0.01	
BfS	1999.9.30	1999.10.1	1	1.38 ± 0.07	
BfS	1999.10.1	1999.10.2	1	1.36 ± 0.01	
BfS	1999.10.2	1999.10.4	2	1.37 ± 0.01	
BfS	1999.10.4	1999.10.12	4	1.47 ± 0.01	
BfS	1999.10.12	1999.10.18	6	1.35 ± 0.01	
BfS	1999.10.18	1999.10.25	4	1.38 ± 0.01	
BfS	1999.10.25	1999.11.1	7	1.39 ± 0.01	
BfS	1999.11.1	1999.11.8	7	1.36 ± 0.01	
BfS	1999.11.8	1999.11.15	7	1.44 ± 0.01	
BfS	1999.11.15	1999.11.22	7	1.38 ± 0.01	
BfS	1999.11.22	1999.11.29	7	1.33 ± 0.01	
BfS	1999.11.29	1999.12.6	7	1.37 ± 0.03	
BfS	1999.12.6	1999.12.13	7	1.44 ± 0.00	
BfS	1999.12.13	1999.12.20	7	1.42 ± 0.01	
BfS	1999.12.20	1999.12.27	7	1.39 ± 0.01	
BfS	1999.12.27	2000.1.3	7	1.37 ± 0.02	
BfS	2000.1.3	2000.1.10	7	1.33 ± 0.01	
BfS	2000.1.10	2000.1.17	7	1.40 ± 0.01	
BfS	2000.1.17	2000.1.24	7	1.39 ± 0.01	
BfS	2000.1.24	2000.1.31	7	1.33 ± 0.01	
BfS	2000.1.31	2000.2.7	7	1.32 ± 0.01	

Table 4.2 Continued

code	start	stop	Duration day	^{85}Kr Bq m^{-3}	remark
BfS	2000.2.7	2000.2.14	7	1.33 ± 0.01	
BfS	2000.2.14	2000.2.21	7	1.35 ± 0.01	
BfS	2000.2.21	2000.2.28	4	1.50 ± 0.01	
BfS	2000.2.28	2000.3.6	7	1.33 ± 0.01	
BfS	2000.3.6	2000.3.13	7	1.39 ± 0.05	
BfS	2000.3.13	2000.3.21	4	1.34 ± 0.01	
BfS	2000.3.21	2000.3.27	6	1.36 ± 0.03	
BfS	2000.3.27	2000.3.31	4	1.36 ± 0.01	
			10	N.A	
MRI_non_anti	2000.4.10	2000.4.17	7	1.39 ± 0.14	
MRI_non_anti	2000.4.17	2000.4.24	7	1.33 ± 0.13	
MRI_non_anti	2000.4.24	2000.5.1	7	1.38 ± 0.14	
MRI_non_anti			7	N.A	
MRI_non_anti	2000.5.8	2000.5.15	7	1.34 ± 0.08	
MRI_non_anti	2000.5.15	2000.5.22	7	1.34 ± 0.12	
MRI_non_anti	2000.5.22	2000.5.29	7	1.24 ± 0.06	
MRI_non_anti	2000.5.29	2000.6.5	7	1.27 ± 0.06	
MRI_non_anti	2000.6.5	2000.6.12	7	1.27 ± 0.06	
MRI_non_anti	2000.6.12	2000.6.19	7	1.27 ± 0.18	
MRI_non_anti	2000.6.19	2000.6.26	7	1.38 ± 0.09	
MRI_non_anti	2000.6.26	2000.7.3	7	1.26 ± 0.05	
MRI_non_anti	2000.7.3	2000.7.10	7	2.35 ± 0.09	
MRI_non_anti	2000.7.10	2000.7.17	7	2.19 ± 0.08	
MRI_non_anti	2000.7.17	2000.7.24	7	2.85 ± 0.12	
MRI_non_anti	2000.7.24	2000.7.31	7	1.24 ± 0.04	
MRI_non_anti	2000.7.31	2000.8.7	7	1.19 ± 0.05	
MRI_non_anti	2000.8.7	2000.8.14	7	1.20 ± 0.06	
MRI_non_anti	2000.8.14	2000.8.21	7	1.29 ± 0.04	
MRI_non_anti	2000.8.21	2000.8.28	7	1.25 ± 0.04	
MRI_non_anti	2000.8.28	2000.9.4	7	1.27 ± 0.04	
MRI_non_anti	2000.9.4	2000.9.11	7	1.23 ± 0.04	
MRI_non_anti	2000.9.11	2000.9.18	7	1.29 ± 0.04	
MRI_non_anti	2000.9.18	2000.9.25	7	1.38 ± 0.06	
MRI_non_anti	2000.9.25	2000.10.2	7	1.33 ± 0.04	
MRI_non_anti	2000.10.2	2000.10.10	8	1.56 ± 0.05	
MRI_non_anti	2000.10.10	2000.10.16	6	1.37 ± 0.06	
MRI_non_anti	2000.10.16	2000.10.23	7	1.39 ± 0.04	
MRI_non_anti	2000.10.23	2000.10.29	6	1.38 ± 0.05	
MRI_non_anti	2000.10.30	2000.11.6	7	1.35 ± 0.07	
MRI_non_anti	2000.11.6	2000.11.13	7	1.47 ± 0.03	
MRI_non_anti	2000.11.13	2000.11.20	7	1.48 ± 0.03	
MRI_non_anti	2000.11.20	2000.11.27	7	1.41 ± 0.02	
MRI_non_anti	2000.11.27	2000.12.4	7	1.63 ± 0.03	
MRI_non_anti	2000.12.4	2000.12.11	7	1.48 ± 0.03	
MRI_non_anti	2000.12.11	2000.12.18	7	1.41 ± 0.03	

Table 4.2 Continued

code	start	stop	Duration day	^{85}Kr Bq m^{-3}	remark
MRI_non_anti	2000.12.18	2000.12.25	7	1.35 ± 0.02	
MRI_non_anti	2000.12.25	2001.1.1	7	1.40 ± 0.02	
MRI_non_anti			8	N.A	
MRI_non_anti	2001.1.9	2001.1.15	6	1.36 ± 0.04	
MRI_non_anti	2001.1.15	2001.1.22	7	1.39 ± 0.04	
MRI_non_anti	2001.1.22	2001.1.29	7	1.39 ± 0.02	
MRI_non_anti	2001.1.29	2001.2.5	7	1.36 ± 0.03	
MRI_non_anti	2001.2.5	2001.2.13	8	1.35 ± 0.03	
MRI_non_anti	2001.2.13	2001.2.19	6	1.34 ± 0.03	
MRI_non_anti	2001.2.19	2001.2.26	7	1.38 ±0.04	
MRI_non_anti	2001.2.26	2001.3.5	7	1.37 ± 0.04	
MRI_non_anti	2001.3.5	2001.3.12	7	1.40 ± 0.02	
MRI_non_anti	2001.3.12	2001.3.19	7	1.66 ± 0.02	
MRI_non_anti	2001.3.19	2001.3.26	7	2.01 ± 0.04	
MRI_non_anti			7	N.A	
MRI_non_anti	2001.4.2	2001.4.9	7	1.39 ± 0.03	
MRI_non_anti	2001.4.9	2001.4.16	7	2.26 ± 0.05	
MRI_non_anti	2001.4.16	2001.4.23	7	2.67 ± 0.04	
MRI_non_anti	2001.4.23	2001.5.1	8	6.36 ± 0.09	
MRI_anti	2001.5.1	2001.5.7	6	1.32 ± 0.03	
MRI_anti	2001.5.7	2001.5.14	7	4.50 ± 0.09	
MRI_anti	2001.5.14	2001.5.21	7	2.23 ± 0.03	
MRI_anti	2001.5.21	2001.5.28	7	2.74 ± 0.04	
MRI_anti	2001.5.28	2001.6.4	7	N.A	
MRI_anti	2001.6.4	2001.6.11	7	1.36 ± 0.01	
MRI_anti	2001.6.11	2001.6.18	7	7.16 ± 0.07	
MRI_anti	2001.6.18	2001.6.25	7	1.36 ± 0.02	
MRI_anti	2001.6.25	2001.7.2	7	1.32 ± 0.02	
MRI_anti	2001.7.2	2001.7.9	7	1.32 ± 0.02	
MRI_anti			7	N.A	
MRI_anti	2001.7.16	2001.7.23	7	1.29 ± 0.02	
MRI_anti	2001.7.23	2001.7.30	7	1.34 ± 0.02	
MRI_anti	2001.7.30	2001.8.6	7	1.36 ± 0.03	
MRI_anti			7	N.A	
MRI_anti	2001.8.13	2001.8.20	7	1.30 ± 0.03	
MRI_anti	2001.8.20	2001.8.27	7	1.32 ± 0.02	
MRI_anti	2001.8.27	2001.9.3	7	1.31 ± 0.02	
MRI_anti	2001.9.3	2001.9.10	7	1.32 ± 0.03	
MRI_anti	2001.9.10	2001.9.17	7	1.32 ± 0.03	
MRI_anti	2001.9.17	2001.9.25	8	1.38 ± 0.03	
MRI_anti	2001.9.25	2001.10.1	6	1.38 ± 0.01	
MRI_anti	2001.10.1	2001.10.9	8	1.38 ± 0.03	
MRI_anti	2001.10.9	2001.10.15	6	3.39 ± 0.06	
MRI_anti	2001.10.15	2001.10.22	7	5.22 ± 0.09	
MRI_anti	2001.10.22	2001.10.28	6	1.57 ± 0.03	

Table 4.2 Continued

code	start	stop	Duration day	^{85}Kr Bq m^{-3}	remark
MRI_anti	2001.10.29	2001.11.5	7	3.16 ± 0.05	
MRI_anti	2001.11.5	2001.11.12	7	1.44 ± 0.02	
MRI_anti	2001.11.12	2001.11.19	7	1.76 ± 0.04	
MRI_anti	2001.11.19	2001.11.26	7	1.49 ± 0.02	
MRI_anti	2001.11.26	2001.12.3	7	2.42 ± 0.04	
MRI_anti	2001.12.3	2001.12.10	7	1.38 ± 0.03	
MRI_anti	2001.12.10	2001.12.17	7	1.40 ± 0.03	
MRI_anti			7	N.A	
MRI_anti	2001.12.24	2001.12.31	7	1.47 ± 0.03	
MRI_anti	2001.12.31	2002.1.7	7	1.46 ± 0.03	
MRI_anti	2002.1.7	2002.1.14	7	1.41 ± 0.04	
MRI_anti	2002.1.14	2002.1.21	7	1.45 ± 0.04	
MRI_anti	2002.1.21	2002.1.28	7	1.49 ± 0.04	
MRI_anti	2002.1.28	2002.2.4	7	1.48 ± 0.05	
MRI_anti	2002.2.4	2002.2.12	8	1.44 ± 0.04	
MRI_anti	2002.2.12	2002.2.18	6	1.48 ± 0.04	
MRI_anti	2002.2.18	2002.2.24	6	1.47 ± 0.05	
MRI_anti	2002.2.25	2002.3.4	7	1.48 ± 0.05	
MRI_anti	2002.3.4	2002.3.11	7	1.45 ± 0.03	
MRI_anti	2002.3.11	2002.3.18	7	1.46 ± 0.04	
MRI_anti	2002.3.18	2002.3.25	7	1.68 ± 0.05	
MRI_anti	2002.3.25	2002.4.1	7	1.60 ± 0.04	
MRI_anti	2002.4.1	2002.4.8	7	4.67 ± 0.11	
MRI_anti	2002.4.8	2002.4.15	7	7.75 ± 0.19	
MRI_anti	2002.4.15	2002.4.22	7	1.57 ± 0.04	
MRI_anti	2002.4.22	2002.4.29	7	4.01 ± 0.13	
MRI_anti	2002.4.29	2002.5.6	7	1.37 ± 0.05	
MRI_anti	2002.5.6	2002.5.13	7	1.47 ± 0.04	
MRI_anti	2002.5.13	2002.5.20	7	9.15 ± 0.21	
MRI_anti	2002.5.20	2002.5.27	7	7.04 ± 0.17	
MRI_anti	2002.5.27	2002.6.3	7	1.77 ± 0.05	
MRI_anti	2002.6.3	2002.6.10	7	1.42 ± 0.04	
MRI_anti	2002.6.10	2002.6.17	7	7.67 ± 0.21	
MRI_anti	2002.6.17	2002.6.24	7	3.49 ± 0.12	
MRI_anti	2002.6.24	2002.7.1	7	1.42 ± 0.03	
MRI_anti	2002.7.1	2002.7.8	7	1.33 ± 0.04	
MRI_anti	2002.7.8	2002.7.15	7	1.31 ± 0.03	
MRI_anti			7	N.A	
MRI_anti	2002.7.22	2002.7.29	7	1.30 ± 0.04	
MRI_anti	2002.7.29	2002.8.5	7	1.26 ± 0.03	
MRI_anti	2002.8.5	2002.8.12	7	1.29 ± 0.04	
MRI_anti	2002.8.12	2002.8.19	7	1.31 ± 0.03	
MRI_anti	2002.8.19	2002.8.26	7	1.36 ± 0.03	
MRI_anti	2002.8.26	2002.9.2	7	1.30 ± 0.03	
MRI_anti	2002.9.9	2002.9.17	7	1.33 ± 0.03	

Table 4.2 Continued

code	start	stop	Duration day	^{85}Kr Bq m^{-3}	remark
MRI_anti	2002.9.17	2002.9.24	7	1.42 ± 0.03	
MRI_anti	2002.9.24	2002.9.30	6	1.42 ± 0.04	
MRI_anti	2002.9.30	2002.10.5	5	1.32 ± 0.03	
MRI_anti	2002.10.7	2002.10.15	8	1.38 ± 0.04	
MRI_anti	2002.10.15	2002.10.22	7	1.40 ± 0.03	
MRI_anti	2002.10.22	2002.10.28	6	3.86 ± 0.10	
MRI_anti	2002.10.28	2002.11.5	8	1.72 ± 0.05	
MRI_anti	2002.11.5	2002.11.11	6	2.35 ± 0.06	
MRI_anti	2002.11.11	2002.11.18	7	1.47 ± 0.04	
MRI_anti	2002.11.18	2002.11.25	7	1.46 ± 0.04	
MRI_anti	2002.11.25	2002.12.2	7	1.48 ± 0.04	
MRI_anti			7	N.A	
MRI_anti	2002.12.9	2002.12.16	7	1.54 ± 0.04	
MRI_anti	2002.12.16	2002.12.24	8	1.46 ± 0.04	
MRI_anti	2002.12.24	2002.12.31	7	1.50 ± 0.04	
MRI_anti			7	N.A	
MRI_anti			7	N.A	
MRI_anti	2003.1.14	2003.1.20	6	1.44 ± 0.04	
MRI_anti	2003.1.20	2003.1.27	7	1.47 ± 0.04	
MRI_anti	2003.1.27	2003.1.27	7	1.44 ± 0.04	
MRI_anti	2003.2.3	2003.2.10	7	1.46 ± 0.04	
MRI_anti	2003.2.10	2003.2.17	7	1.45 ± 0.04	
MRI_anti	2003.2.17	2003.2.24	7	1.40 ± 0.03	
MRI_anti	2003.2.24	2003.3.3	7	1.40 ± 0.03	
MRI_anti	2003.3.3	2003.3.10	7	1.42 ± 0.04	
MRI_anti	2003.3.10	2003.3.17	7	1.44 ± 0.04	
MRI_anti	2003.3.17	2003.3.24	7	1.49 ± 0.04	
MRI_anti	2003.3.24	2003.3.31	7	1.40 ± 0.03	
MRI_anti	2003.3.31	2003.4.7	7	1.44 ± 0.04	
MRI_anti	2003.4.7	2003.4.14	7	1.42 ± 0.03	
MRI_anti	2003.4.14	2003.4.21	7	1.42 ± 0.03	
MRI_anti	2003.4.21	2003.4.28	7	1.48 ± 0.04	
MRI_anti	2003.4.28	2003.5.6	8	1.49 ± 0.04	
MRI_anti	2003.5.6	2003.5.12	6	1.44 ± 0.04	
MRI_anti	2003.5.12	2003.5.19	7	1.51 ± 0.04	
MRI_anti	2003.5.19	2003.5.26	7	1.52 ± 0.04	
MRI_anti	2003.5.26	2003.6.2	7	1.50 ± 0.05	
MRI_anti	2003.6.2	2003.6.9	7	1.51 ± 0.04	
MRI_anti	2003.6.9	2003.6.16	7	1.47 ± 0.03	
MRI_anti	2003.6.16	2003.6.23	7	1.41 ± 0.03	
MRI_anti	2003.6.23	2003.6.30	7	1.40 ± 0.02	
MRI_anti	2003.6.30	2003.7.7	7	1.41 ± 0.02	
MRI_anti	2003.7.7	2003.7.14	7	1.42 ± 0.03	
MRI_anti	2003.7.14	2003.7.22	8	1.44 ± 0.02	
MRI_anti	2003.7.22	2003.7.28	6	1.40 ± 0.02	

Table 4.2 Continued

code	start	stop	Duration day	^{85}Kr Bq m^{-3}	remark
MRI_anti	2003.7.28	2003.8.4	7	1.39 ± 0.02	
MRI_anti	2003.8.4	2003.8.11	7	1.33 ± 0.02	
MRI_anti	2003.8.11	2003.818	7	1.40 ± 0.02	
MRI_anti	2003.8.18	2003.8.25	7	1.37 ± 0.02	
MRI_anti	2003.8.25	2003.9.1	7	1.34 ± 0.03	
MRI_anti	2003.9.1	2003.9.8	7	1.39 ± 0.03	
MRI_anti	2003.9.8	2003.9.16	8	1.34 ± 0.03	
MRI_anti	2003.9.16	2003.9.22	6	1.79 ± 0.02	
MRI_anti	2003.9.22	2003.9.29	7	3.71 ± 0.04	
MRI_anti	2003.9.29	2003.10.6	7	3.75 ± 0.06	
MRI_anti	2003.10.6	2003.10.14	8	4.33 ± 0.05	
MRI_anti	2003.10.14	2003.10.20	6	1.44 ± 0.01	
MRI_anti	2003.10.20	2003.10.27	7	5.91 ± 0.06	
MRI_anti	2003.10.27	2003.11.4	8	2.53 ± 0.03	
MRI_anti	2003.11.4	2003.11.10	6	2.95 ± 0.03	
MRI_anti	2003.11.10	2003.11.17	7	4.28 ± 0.04	
MRI_anti	2003.11.17	2003.11.25	8	1.48 ± 0.01	
MRI_anti	2003.11.25	2003.12.1	6	1.44 ± 0.01	
MRI_anti	2003.12.1	2003.12.8	7	1.45 ± 0.01	
MRI_anti	2003.12.8	2003.12.15	7	1.46 ± 0.01	
MRI_anti	2003.12.15	2003.12.22	7	1.48 ± 0.03	
MRI_anti	2003.12.22	2003.12.26	4	1.48 ± 0.01	
MRI_anti			10	N.A	
MRI_anti	2004.1.5	2004.1.13	8	1.51 ± 0.02	
MRI_anti	2004.1.13	2004.1.19	6	1.49 ± 0.01	
MRI_anti	2004.1.19	2004.1.25	6	1.53 ± 0.01	
MRI_anti	2004.1.26	2004.2.2	7	3.01 ± 0.04	
MRI_anti	2004.2.2	2004.2.9	7	1.92 ± 0.01	
MRI_anti	2004.2.9	2004.2.16	7	1.69 ± 0.01	
MRI_anti	2004.2.16	2004.2.21	5	1.59 ± 0.01	
MRI_anti	2004.2.23	2004.3.1	7	2.58 ± 0.03	
MRI_anti	2004.3.1	2004.3.8	7	1.72 ± 0.02	
MRI_anti	2004.3.8	2004.3.15	7	1.66 ± 0.03	
MRI_anti	2004.3.15	2004.3.22	7	2.16 ± 0.02	
MRI_anti	2004.3.22	2004.3.29	7	1.51 ± 0.02	
MRI_anti	2004.3.29	2004.4.5	7	1.86 ± 0.02	
MRI_anti	2004.4.5	2004.4.12	7	2.01 ± 0.02	
MRI_anti	2004.4.12	2004.4.19	7	2.63 ± 0.02	
MRI_anti	2004.4.19	2004.4.26	7	1.49 ± 0.01	
MRI_anti	2004.4.26	2004.5.3	7	1.83 ± 0.02	
MRI_anti	2004.5.3	2004.5.11	8	1.47 ± 0.03	
MRI_anti	2004.5.11	2004.5.17	6	2.73 ± 0.03	
MRI_anti	2004.5.17	2004.5.24	7	5.45 ± 0.06	
MRI_anti	2004.5.24	2004.5.31	7	1.57 ± 0.03	
MRI_anti	2004.5.31	2004.6.7	7	1.54 ± 0.03	

Table 4.2 Continued

code	start	stop	Duration day	^{85}Kr Bq m^{-3}	remark
MRI_anti	2004.6.7	2004.6.14	7	1.47 ± 0.03	
MRI_anti	2004.6.14	2004.6.21	7	1.49 ± 0.01	
MRI_anti	2004.6.21	2004.6.28	7	1.40 ± 0.02	
MRI_anti	2004.6.28	2004.7.5	7	1.45 ± 0.02	
MRI_anti	2004.7.5	2004.7.12	7	1.38 ± 0.02	
MRI_anti	2004.7.12	2004.7.20	8	1.43 ± 0.01	
MRI_anti	2004.7.20	2004.7.26	6	1.40 ± 0.02	
MRI_anti	2004.7.26	2004.8.2	7	1.39 ± 0.01	
MRI_anti	2004.8.2	2004.8.9	7	1.39 ± 0.02	
MRI_anti	2004.8.9	2004.8.16	2	1.44 ± 0.01	
MRI_anti	2004.8.16	2004.8.23	4	1.43 ± 0.01	
MRI_anti	2004.8.23	2004.8.30	7	1.46 ± 0.01	
MRI_anti	2004.8.30	2004.9.6	7	1.40 ± 0.01	
MRI_anti	2004.9.6	2004.9.13	7	1.41 ± 0.01	
MRI_anti	2004.9.13	2004.9.21	7	1.46 ± 0.01	
MRI_anti	2004.9.21	2004.9.27	8	1.47 ± 0.01	
MRI_anti	2004.9.27	2004.10.4	7	1.47 ± 0.01	
MRI_anti	2004.10.4	2004.10.12	8	2.32 ± 0.02	
MRI_anti	2004.10.12	2004.10.18	6	7.12 ± 0.06	
MRI_anti	2004.10.18	2004.10.25	7	4.51 ± 0.03	
MRI_anti	2004.10.25	2004.11.1	7	5.74 ± 0.04	
MRI_anti	2004.11.1	2004.11.8	7	1.48 ± 0.01	
MRI_anti	2004.11.8	2004.11.15	7	3.70 ± 0.03	
MRI_anti	2004.11.15	2004.11.22	7	2.27 ± 0.02	
MRI_anti	2004.11.22	2004.11.29	7	1.45 ± 0.01	
MRI_anti	2004.11.29	2004.12.6	7	1.52 ± 0.01	
MRI_anti	2004.12.6	2004.12.13	7	1.55 ± 0.02	
MRI_anti	2004.12.13	2004.12.20	7	1.54 ± 0.01	
MRI_anti	2004.12.20	2004.12.24	4	1.57 ± 0.01	
MRI_anti	2004.12.24	2005.1.4	11	1.52 ± 0.01	
MRI_anti	2005.1.4	2005.1.11	7	1.45 ± 0.02	
MRI_anti	2005.1.11	2005.1.17	6	1.51 ± 0.02	
MRI_anti	2005.1.17	2005.1.24	7	1.50 ± 0.01	
MRI_anti	2005.1.24	2005.1.31	7	1.51 ± 0.01	
MRI_anti	2005.1.31	2005.2.7	7	1.52 ± 0.01	
MRI_anti	2005.2.7	2005.2.14	7	2.59 ± 0.03	
MRI_anti	2005.2.14	2005.2.21	7	2.44 ± 0.03	
MRI_anti	2005.2.21	2005.2.28	7	3.20 ± 0.03	
MRI_anti	2005.2.28	2005.3.7	7	1.49 ± 0.01	
MRI_anti	2005.3.7	2005.3.14	7	9.83 ± 0.08	
MRI_anti	2005.3.14	2005.3.22	8	6.21 ± 0.05	
MRI_anti	2005.3.22	2005.3.28	6	1.64 ± 0.01	
MRI_anti	2005.3.28	2005.4.4	7	1.52 ± 0.01	
MRI_anti	2005.4.4	2005.4.11	7	1.78 ± 0.02	
MRI_anti	2005.4.11	2005.4.18	7	3.61 ± 0.03	

Table 4.2 Continued

code	start	stop	Duration day	^{85}Kr Bq m^{-3}	remark
MRI_anti	2005.4.18	2005.4.25	7	4.33 ± 0.03	
MRI_anti	2005.4.25	2005.5.2	7	1.55 ± 0.01	
MRI_anti	2005.5.2	2005.5.9	7	1.53 ± 0.01	
MRI_anti	2005.5.9	2005.5.16	7	3.42 ± 0.03	
MRI_anti	2005.5.16	2005.5.23	7	2.91 ± 0.02	
MRI_anti	2005.5.23	2005.5.30	7	4.47 ± 0.05	
MRI_anti	2005.5.30	2005.6.6	7	1.49 ± 0.01	
MRI_anti	2005.6.6	2005.6.13	7	1.49 ± 0.01	
MRI_anti	2005.6.13	2005.6.20	7	1.47 ± 0.01	
MRI_anti	2005.6.20	2005.6.27	7	1.45 ± 0.01	
MRI_anti	2005.6.27	2005.7.4	7	1.41 ± 0.01	
MRI_anti	2005.7.4	2005.7.11	7	1.44 ± 0.02	
MRI_anti	2005.7.11	2005.7.19	8	1.44 ± 0.01	
MRI_anti	2005.7.19	2005.7.25	6	1.47 ± 0.02	
MRI_anti	2005.7.25	2005.8.1	7	1.41 ± 0.01	
MRI_anti	2005.8.1	2005.8.8	7	1.37 ± 0.01	
MRI_anti	2005.8.8	2005.8.15	7	1.40 ± 0.01	
MRI_anti	2005.8.15	2005.8.22	7	1.40 ± 0.02	
MRI_anti	2005.8.22	2005.8.29	7	1.41 ± 0.02	
MRI_anti	2005.8.29	2005.9.5	7	1.43 ± 0.02	
MRI_anti	2005.9.5	2005.9.12	7	1.40 ± 0.02	
MRI_anti	2005.9.12	2005.9.20	18	1.40 ± 0.02	
MRI_anti	2005.9.20	2005.9.26	6	1.43 ± 0.02	
MRI_anti	2005.9.26	2005.10.3	7	1.51 ± 0.03	
MRI_anti	2005.10.3	2005.10.7	4	1.55 ± 0.02	
MRI_anti	2005.10.7	2005.10.17	10	2.42 ± 0.02	
MRI_anti	2005.10.17	2005.10.24	7	2.50 ± 0.03	
MRI_anti	2005.10.24	2005.10.31	7	5.11 ± 0.05	
MRI_anti	2005.10.31	2005.11.7	7	2.24 ± 0.02	
MRI_anti	2005.11.7	2005.11.14	7	1.57 ± 0.02	
MRI_anti	2005.11.14	2005.11.21	7	3.38 ± 0.04	
MRI_anti	2005.11.21	2005.11.28	7	3.03 ± 0.04	
MRI_anti	2005.11.28	2005.12.5	7	1.80 ± 0.02	
MRI_anti	2005.12.5	2005.12.12	7	1.58 ± 0.02	
MRI_anti	2005.12.12	2005.12.19	7	1.53 ± 0.02	
MRI_anti	2005.12.19	2005.12.26	7	1.52 ± 0.02	
MRI_anti	2005.12.26	2006.1.4	9	1.50 ± 0.02	
MRI_anti	2006.1.4	2006.1.10	6	1.46 ± 0.02	
MRI_anti	2006.1.10	2006.1.16	6	1.51 ± 0.02	
MRI_anti	2006.1.16	2006.1.23	7	1.52 ± 0.02	
MRI_anti	2006.1.23	2006.1.0	7	1.62 ± 0.02	
MRI_anti	2006.1.30	2006.2.6	7	1.51 ± 0.02	
MRI_anti	2006.2.6	2006.2.13	7	1.62 ± 0.02	
MRI_anti	2006.2.13	2006.2.20	7	2.99 ± 0.03	
MRI_anti	2006.2.20	2006.2.27	7	8.19 ± 0.08	

Table 4.2 Continued

code	start	stop	Duration day	^{85}Kr Bq m^{-3}	remark
MRI_anti	2006.2.27	2006.3.6	7	3.18 ± 0.03	
MRI_anti	2006.3.6	2006.3.13	7	1.52 ± 0.02	

*mean of two or more measurements
** minican was empty

4.2 Results in Tsukuba and Chiba during the technical transfer

The collection of the air samples in Tsukuba (MRI) and in Chiba (JCAC) from January 2006 has been started according to the technical transfer schedule. At the beginning, the air samples were collected only in Tsukuba. On the other hand, the air sampling in Chiba has been started at the end of February 2006 after the sampling unit was transferred to Chiba.

In order to guarantee the continuity of the data for the atmospheric ^{85}Kr activity concentration in Japan, the air samples both in Tsukuba and in Chiba were collected for one month in April 2006, and the atmospheric ^{85}Kr activity concentrations were compared with each other. The results of to the atmospheric ^{85}Kr activity concentration at two sampling points are presented in Table 4.3 and Fig. 4.5.

When we compared the atmospheric ^{85}Kr activity concentration in Tsukuba and that in Chiba when Tokai plant was not operating, the atmospheric ^{85}Kr activity concentration in Tsukuba (1.48-1.41 Bq m^{-3} in Jan., 2006) coincided with that in Chiba (1.47-1.48 Bq m^{-3} in May, 2006) within the counting error. The finding concluded that no significant difference exiated between the atmospheric ^{85}Kr activity concentrations in Chiba and that in Tsukuba, although Chiba is located 60 km from Tsukuba.

Table 4.3 Atmospheric ^{85}Kr activity concentration in Tsukuba and in Chiba

code	start	stop	Duration in days	^{85}Kr activity concentration In Bq m^{-3}	
				Tsukuba	Chiba
MRI	2006.1.5	2006.1.10	5	1.49 ± 0.01	-
MRI	2006.1.18	2006.1.25	7	1.49 ± 0.01	-
MRI	2006.1.25	2006.2.1	7	1.48 ± 0.01	-
MRI	2006.2.1	2006.2.8	7	1.49 ± 0.01	-
MRI	2006.2.8	2006.2.15	7	1.61 ± 0.01	-
MRI	2006.2.28	2006.3.7	7	-	2.24 ± 0.02
MRI	2006.3.7	2006.3.14	7		1.49±0.01
MRI	2006.3.14	2006.3.22	8		1.85±0.02
MRI	2006.3.22	2006.3.28	6		2.04±0.02
MRI	2006.3.28	2006.4.4	7		1.53±0.01
MRI	2006.4.4	2006.4.11	7	2.29±0.02	1.59±0.01
MRI	2006.4.11	2006.4.17	6	3.01±0.03	2.03±0.02
MRI	2006.4.17	2006.4.24	7	2.84±0.02	1.56±0.01
MRI	2006.4.24	2006.5.2	8		1.64±0.01
MRI	2006.5.2	2006.5.6	4		1.48±0.04
MRI	2006.5.11	2006.5.15	4		1.47±0.04
MRI	2006.5.15	2006.5.23	8		1.46±0.02
MRI	2006.5.23	2006.5.30	7		1.48±0.02
JCAC	2006.5.30	2006.6.6	7		1.47±0.02
JCAC	2006.6.6	2006.6.13	7		1.49±0.02
JCAC	2006.6.13	2006.6.20	7		1.42±0.02
JCAC	2006.6.20	2006.6.28	8		1.44±0.02
JCAC	2006.6.28	2006.7.3	5		1.40±0.03

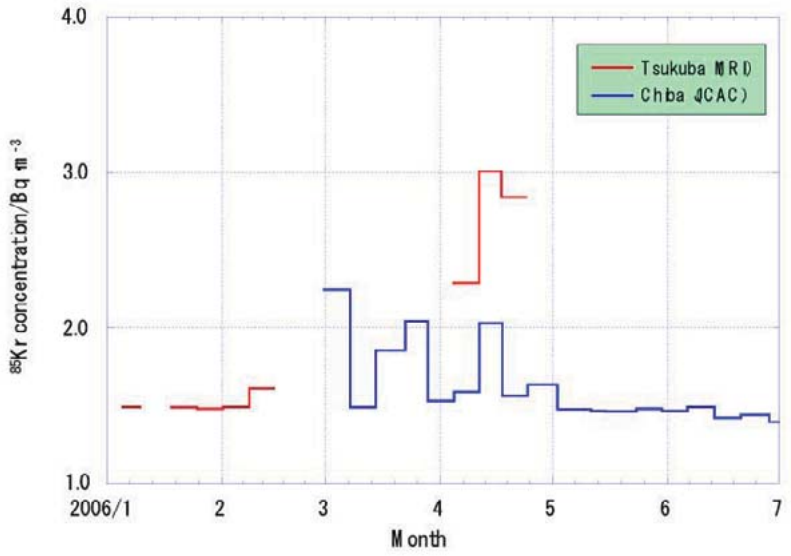

Figure 4.5 Temporal variation of atmospheric ^{85}Kr activity concentration in Tsukuba and in Chiba

Compared with the background level (1.5 Bq m^{-3}) of the atmospheric ^{85}Kr in Japan (Tsukuba), relatively high ^{85}Kr activity concentrations in Tsukuba and Chiba were observed from March to April 2006. The air samples were collected both in Tsukuba and in Chiba during three weeks from the beginning of April 2006, and the observed concentrations of the atmospheric ^{85}Kr in Tsukuba were generally higher than those in Chiba. The reason why the concentration of the atmospheric ^{85}Kr became higher than background level is considered to be the influence of the operation of the nuclear fuel reprocessing plant at Tokai, which is located about 60 km northeast of Tsukuba. Although the transport of ^{85}Kr from Tokai to sampling sites depends on the meteorological conditions (wind direction and wind velocity), previous analysis (Igarashi et al., 2000) revealed that the discharged ^{85}Kr by the reprocessing of spent nuclear fuel caused temporal increase of the atmospheric ^{85}Kr activity concentration in Tsukuba. In addition, the reason why the concentrations of the atmospheric ^{85}Kr in Tsukuba were higher than those in Chiba is

explained by the difference of the distances of two sampling sites from the reprocessing plant at Tokai. Since Chiba is located about 100 km away from Tokai, it was expected that the influence on the atmospheric ^{85}Kr activity concentrations in Chiba due to the ^{85}Kr release from the Tokai nuclear reprocessing plant would be less than that in Tsukuba.

4.3 Atmospheric ^{85}Kr activity concentrations in Aomori

The operation of the large-scale nuclear fuel reprocessing plant started in April 2006 at Rokkasho, Aomori in northern area of the Honshu Island. As a result, a significant amount of ^{85}Kr will be released into the atmosphere. Therefore, it is important to know the background level of the atmospheric ^{85}Kr activity concentration in Aomori before the operation of the plant. We continuously collected weekly air samples at Aomori (40º 49' N, 140º 45' E) during the period from June 2003 to March 2006.

The temporal variation of the ^{85}Kr activity concentration in surface air in Aomori is showen in Fig. 4.6. The ^{85}Kr activity concentrations in Aomori in June to December 2003 were 1.38 to 1.58 Bq m^{-3}, those in 2004 were 1.39 to 1.66 Bq m^{-3}, those in 2005 were 1.39 to 1.66 Bq m^{-3} and those in January to March 2006 were 1.50 to 1.77 Bq m^{-3}, respectively. The atmospheric ^{85}Kr activity concentrations in Aomori were generally slightly higher than those in Tsukuba. The ^{85}Kr cactivity oncentration in Aomori showed a seasonal change with high in winter and low in summer as observed in Tsukuba. During this period, the ^{85}Kr activity concentration in both Aomori and Tsukuba gradually increased.

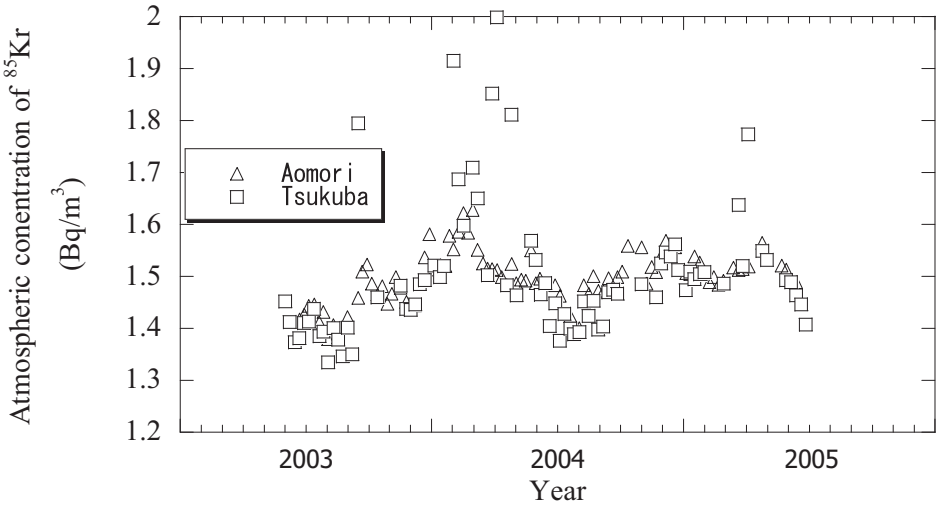

Figure 4.6 Background ^{85}Kr activity concentration observed at Tsukuba and Aomori during 2003 to 2005 (Geochemical Res. Dep., MRI, 2005, pages 36, Figure 2)

4.4 ^{85}Kr activity at several sites in Japan

In order to clarify the spatial distribution of the atmospheric ^{85}Kr activity concentrations in Japan, we collected air samples at six stations of Japan during the period from 1995 to 2001. However, the data of the atmospheric ^{85}Kr in the six stations (Table 4.4), except Tsukuba, are scant. Therefore we introduced normalized ^{85}Kr activity concentrations. All the background data observed from 1995 to 2001 at all the stations in Japan were normalized to the concentration level of 2001 taking into account the annual growth rate of 0.03 Bq m^{-3} yr^{-1}; this enabled us to obtain information about the spatial distribution of the background atmospheric ^{85}Kr activity concentrations regardless of the annual variations. Figure 4.7 depicts the seasonal variations of the normalized atmospheric ^{85}Kr activity concentrations in Tsukuba together with those observed at the six stations over the Japanese islands. As shown in Fig. 4.7, the atmospheric ^{85}Kr activity concentrations from February to March at the stations of Wak-kanai, Sapporo, Osaka and Ishigaki were at the same levels as those in Tsukuba. On the other hand, a few data obtained in December in

Sapporo and Ishigaki seem to be different from those in Tsukuba, which is explained as follows. Since Sapporo is at a higher latitude than Tsukuba, it was covered in early winter by the continental air mass directly affected by European sources. Therefore the ^{85}Kr activity concentrations in Sapporo were higher than in Tsukuba in December. On the other hand, Ishigaki, at a lower latitude than Tsukuba, was still covered by the Pacific air mass with lower ^{85}Kr; thus the ^{85}Kr activity concentrations in Ishigaki were lower than in Tsukuba. It is suggested that the atmospheric ^{85}Kr activity concentrations in early winter in Japan reflect global-scale latitudinal gradient (Weiss et al., 1992). On the other hand, in winter to early spring, Japanese islands were covered by the continental air mass.

Table 4.4 Sampling locations and related information.

Station	Location	Sampling period	Frequency of sampling	Height of intake
Tsukuba	36.05°N, 140.13°E	1 week	every week	40 m
Sapporo	43.06°N, 141.33°E	3 days	once a year	17.2 m
Ishigaki	24.33°N, 124.16°E	3 days	once a year	5.7 m
Wakkanai	45.41°N, 141.68°E	2 hours	once a year	10.6 m
Sendai	38.26°N, 140.90°E	2 hours	once a year	38.9 m
Osaka	34.68°N, 135.52°E	2 hours	once a year	92.6 m
Fukuoka	33.58°N, 130.38°E	2 hours	once a year	17.1 m

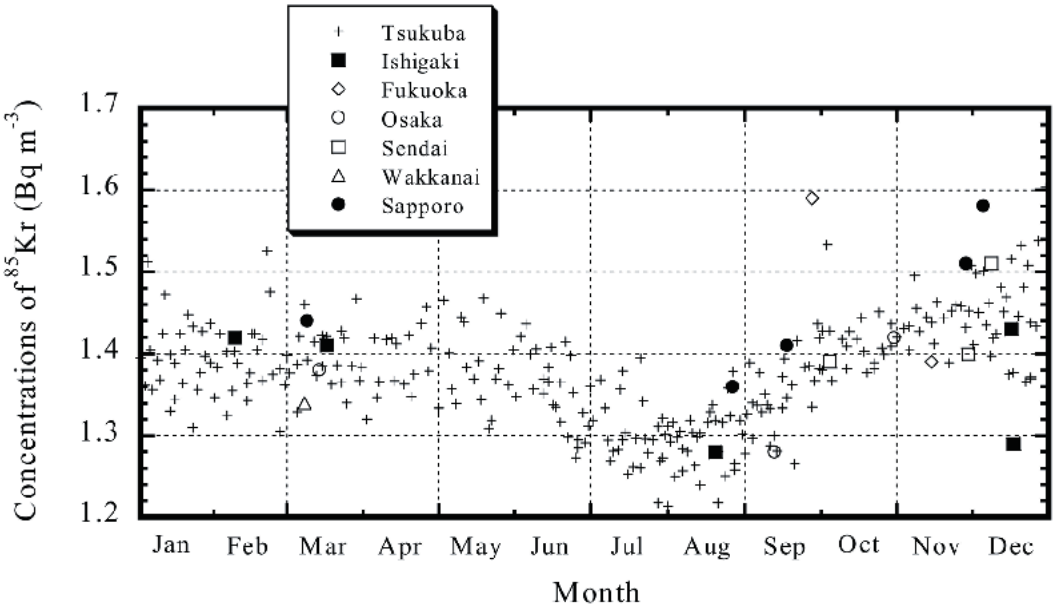

Figure 4.7 Seasonal variation of the atmospheric ^{85}Kr activity concentrations at all stations in Japan. Data were obtained for the period from 1995 to 2001. All data were normalized to the concentration levels of 2001 on the assumption of an annual growth rate of 0.03 Bq·m^{-3}·yr^{-1}. (Hirota et al., 2004, Figure 7)